Physica D 461 (2024) 134125

Contents lists available at ScienceDirect

Physica D

journal homepage: www.elsevier.com/locate/physd

Homogeneous and heterogeneous nucleation in the three-state Blume–Capel model

Emilio N.M. Cirillo [a], Vanessa Jacquier [b,*], Cristian Spitoni [b]

[a] Dipartimento di Scienze di Base e Applicate per l'Ingegneria Sapienza Università di Roma, via A. Scarpa 16, I 00161, Roma, Italy
[b] Institute of Mathematics, University of Utrecht, Budapestlaan 6, 3584 CD, Utrecht, The Netherlands

ARTICLE INFO

Communicated by V.M. Perez-Garcia

Keywords:
Glauber dynamics
Blume–Capel model
Metastability
Nucleation
Low temperature dynamics
Effect of boundary conditions

ABSTRACT

We study metastability in a three-state lattice spin system in presence of zero-boundary condition, which is a relevant choice from the point of view of applications, since it mimics the presence of defects in the system. This problem is studied in the framework of the stochastic Blume–Capel model with Glauber dynamics and it is proven that the presence of zero-boundary conditions changes drastically the metastability scenarios. In particular we show that, depending on the parameters of the model, the stable phase nucleation can be either homogeneous or heterogeneous. Notably, heterogeneous nucleation is proved in the region of the parameter space where the chemical potential is larger than the external magnetic field.

1. Introduction

We study the metastable behavior of the stochastic Blume–Capel model [1,2] under the Glauber dynamics with zero-boundary conditions.

This model represents, together with the Potts model, a paradigmatic example of multi-state spin systems and a natural generalization of the two-state Ising model. Moreover, it has been considered in the literature for several applications in different fields. It was originally introduced to study the ^{3}He-^{4}He transition, but, thanks to the richness of its behaviors, in more recent years it has been exploited to address several problems, such as the spinodal decomposition in presence of solvent [3,4], with potential application to solar cell technologies, and to biological systems, for instance, the study of the ground states of DNA molecule [5].

In the framework of the spinodal decomposition problem the Blume–Capel model has shown its ability to describe the formation of patterns of three different phases. This is achieved essentially by a sudden quench to a subcritical temperature of an infinite temperature state, namely, a completely randomly chosen configuration. In this paper we shall analyze the behavior of the model in a completely different regime, indeed the low temperature and the presence of an external field will ensure the existence of a unique equilibrium state and we shall describe how the system, starting from a non-equilibrium metastable state, will perform the transition to the stable one via the nucleation of a critical droplet, achieved by means of a long series of random fluctuations. In particular, we shall study the effect of the boundary conditions on this nucleation process.

As we shall discuss below, the Blume–Capel model, in this metastable regime, shows an amazing variety of nucleation processes that might inspire future generalizations to more mathematically treatable complex model, closer to the *Cellular Potts Model* [6,7]. The Cellular Potts Models (CPM) represent indeed a popular and successful method for modeling collective cell behavior during *tumor development*: e.g., *cell sorting*, *gastrulation*, or *angiogenesis*. This dynamics presents different time scales and, in some regions of the parameter space, metastability shows up.

The metastable behavior of the Blume–Capel model has been firstly rigorously studied in [8] in finite volume in the limit of temperature tending to zero. In that paper the parameters have been chosen so that the metastable state is unique. The same regime is studied in [9–11], where the parameters are chosen in such a way that the model has two non-degenerate in energy metastable states [12]. The infinite volume regime was considered in [13,14]. The study of the metastability for three different types of spins, $-1, 0, +1$ has similarities with the two types of particles 1, 2 and the *empty space* (0) in [15], where the authors study the evolution of the system under Kawasaki dynamics.

We recall, also, that the metastable behavior of the Blume–Capel model has been studied at finite temperature via non-rigorous methods, such as the transfer–matrix method and the Monte Carlo simulations, in several papers, see, for instance, the classical Ref. [16] and the

* Corresponding author.
E-mail addresses: emilio.cirillo@uniroma1.it (E.N.M. Cirillo), v.jacquier@uu.nl (V. Jacquier), C.Spitoni@uu.nl (C. Spitoni).

https://doi.org/10.1016/j.physd.2024.134125
Received 3 November 2023; Received in revised form 14 January 2024; Accepted 2 March 2024
Available online 5 March 2024

more recent [17] where the anisotropic case has been approached. We mention, also, the useful review [18] for a complete report on the numerical approaches to metastable states.

Metastability is a widely studied phenomenon that has been investigated on mathematical grounds over the last fifty years from different points of view and with several approaches. We will use, here, the so-called *pathwise approach*, originally proposed in [19] and then developed in several more recent studies [20–23]. This method provides a standard way of characterizing metastable states and a technique to compute their exit time and to describe the typical exit trajectories.

Two other approaches to the rigorous mathematical description of metastability have been developed in recent decades, the *potential-theoretic approach* [24–26] and the *trace method* [27].

The study of metastability is typically carried out for periodic boundary conditions; indeed, these are a rather natural setting in this context. In particular periodic boundary condition have been considered in all the above mentioned studies of the Blume–Capel model. In the present paper we will consider the case of zero-boundary condition, which is particularly important from the point of view of applications, because non-periodic boundary conditions mimic the presence of defects or boundaries in the system.

In the presence of defects (or boundaries), the nucleus of the new phase forms in contact with the impurities (or boundaries), so that the properties of the impurities control the nucleation rate. Indeed, the nucleation starts at phase boundaries or impurities, since at these sites the free energy barrier is lower, and the nucleation is facilitated. Therefore, the nucleation observed in practice is usually catalyzed and it is called *heterogeneous nucleation*: see for instance [28,29] for the crystallization case, and [30] for the condensation.

In order to understand the general mechanisms triggering the heterogeneous nucleation, Monte Carlo simulations for simple toy models (e.g., Ising and lattice gas models) are often used, see [31]. For instance, in [32] Monte Carlo simulations for two-dimensional Ising models are used to study the role of *pores* on the surface in the nucleation process. The simulations show that the nucleation occurring at pores has a nucleation rate that is of orders of magnitude higher than that starting on flat surfaces. This behavior is very common for porous materials, which in fact often exhibit the well-known phenomenon of *capillary condensation*, i.e., the condensation of liquid bridges in the pores, see [33].

Simulations of two dimensional Ising model have also been used to study the role of microscopic impurities (i.e., sites with fixed spins) in the bulk [34]: the heterogeneous nucleation, starting from a single fixed spin, is more than four orders of magnitude faster than homogeneous nucleation. Therefore, small microscopic impurities strongly promote nucleation, making it very difficult to purify a sample sufficiently in order to observe homogeneous nucleation. The same conclusions are also obtained as well for the two-dimensional Potts model [35] with competitive nucleating phases.

Heterogeneous nucleation also plays a pivotal role in the process of *crystallization of proteins* on surfaces (see [36]): by tuning the geometrical properties of the surface (porosity, pore size, roughness), heterogeneous nucleation can be activated, enhancing the probability of obtaining crystals of appropriate size. The paper [37] uses a two-dimensional Ising model to show the dependence of the nucleation rate on the polymeric surfaces used as substrate for heterogeneous nucleation. Indeed, Different rough surfaces are modeled with different profiles of fixed spins at the boundaries.

The effect of the boundary conditions on the metastable behavior has been rigorously studied in [38] in the framework of the Ising model; there the free boundary condition case was considered. The authors proved that the main features characterizing the metastable behavior in the case of periodic boundary conditions remain unchanged. However, some new effects appear: the main difference with the periodic case is that the nucleation phenomenon is no more spatially homogeneous, in the sense that the critical droplet, that must be formed to nucleate the stable state, necessarily occurs at one of the four corners of the lattice. Other details, such as the size of the critical droplet, are different and hence the exponential estimate of the exit time.

In this paper we will show that, due to the three-state character of the Blume–Capel model, the metastability scenario proven for periodic boundary conditions [8] changes deeply when different boundary conditions are considered.

The Hamiltonian of the Blume–Capel model depends on two parameters, the magnetic field h and the chemical potential λ. The spin variables can take three values, -1, 0, and $+1$. We limit our discussion to the case $\lambda, h > 0$, where the chemical potential term favors minus and plus spins equally with respect to the zeros and the magnetic field favors pluses and disadvantages minuses with respect to the zeros. In this parameter region, in the periodic case, the following result was proved in [8] (see Fig. 1 for a schematic description): the stable state is the homogeneous plus state and the metastable state is the homogeneous minus state. Furthermore, for $h > 2\lambda$ the system exits the metastable state by forming a zeros square droplet and reaches the homogeneous zero state. Then, at a random time the transition from the zero state to the stable state is realized via the formation of a plus square droplet. For $2\lambda > h$ the system exits the metastable state by forming a plus square droplet separated from the sea of minuses by a layer of zeros of width one (with minus at the corners in the case $\lambda > h$). In this way the stable state is reached directly.

This scenario changes drastically when zero-boundary conditions are considered: for $h > \lambda$ the metastable state is the homogeneous zero state and the plus stable state is reached via the formation of a plus square droplet at any point in the lattice. For $\lambda > h$, on the other hand, the situation is similar to the periodic boundary condition case, but, starting from the minus metastable state, the stable phase is nucleated at one of the four corners of the lattice via the formation of a plus square droplet separated from the sea of minus by a one site zero layer. Thus, the nucleation is spatially homogeneous for $h > \lambda$ and spatially non-homogeneous for $\lambda > h$. This scenario is rigorously proven in the $\lambda > h > \lambda/2$ region of the parameter plane.

The paper is organized as follows. In Section 2 we introduce the model and discuss some preliminary properties. In Section 3.1 we present the heuristic study of the metastable behavior of the model in the parameter region $h, \lambda > 0$ and in Section 3.2 we state our rigorous results for the restricted region $\lambda > h > \lambda/2$. Section 4 is devoted to the proof of the results given in Sections 2 and 3.2. Our conclusions are summarized in Section 5. The proofs of the technical lemmas are reported in Appendix.

2. Model and definitions

In this section we define the model and we give some definitions and preliminary results. Proofs are postponed to Section 4.

2.1. The lattice

We consider the set $\mathbb{Z}^2$ embedded in $\mathbb{R}^2$ and call *sites* its elements. Given two sites $i, i' \in \mathbb{Z}^2$ we let $|i - i'|$ be their Euclidean distance. Given $i \in \mathbb{Z}^2$, we say that $i' \in \mathbb{Z}^2$ is a *nearest neighbor* of i if and only if $|i - i'| = 1$. Pairs of neighboring sites will be called *bonds*. A set $I \subset \mathbb{Z}^2$ is *connected* if and only if for any $i \neq i' \in I$ there exists a sequence $i_1, i_2, \dots, i_n$ of sites of I such that $i_1 = i$, $i_n = i'$, and i_k and i_{k+1} are nearest neighbors for any $k = 1, \dots, n-1$.

A *column*, resp. a *row*, of $\mathbb{Z}^2$ is a sequence of L connected sites of Λ such that the line joining them is parallel to the vertical, resp. horizontal, axis.

Given $I \subset \mathbb{Z}^2$ we call *internal boundary* $\partial^- I$ of I the set of sites in I having a nearest neighbor outside I. The *bulk* of I is the set $I \setminus \partial^- I$, namely, the set of sites of I having four nearest neighbors in I. We call *external boundary* $\partial^+ I$ of I the set of sites in $\mathbb{Z}^2 \setminus I$ having a nearest neighbor in I.

A set $R \subset \mathbb{Z}^2$ is called a *rectangle* (resp. *square*) if the union of the closed unit squares of $\mathbb{R}^2$ centered in the sites of R with sides parallel to the axes of $\mathbb{Z}^2$ is a rectangle (resp. a square) of $\mathbb{R}^2$. The *sides* of a rectangle are the four maximal connected subsets of its internal boundary (note that they lie on straight lines parallel to the axes of $\mathbb{Z}^2$). The *length* of one side of a rectangle is the number of sites belonging to the side itself. A *quasi-square* is a rectangle with side lengths equal to n and $n+1$, with n an integer greater than or equal to one.

For any set $I \subset \mathbb{Z}^2$ we call *rectangular envelope* of I the smallest (with respect to inclusion) rectangle $R \subset \mathbb{Z}^2$ such that $I \subset R$. Two rectangles of $\mathbb{Z}^2$ are called *interacting* if their mutual distance is smaller than or equal to 2, that is to say, either their intersection is not empty or there exist two neighboring sites belonging one to the first rectangle and the other one to the second rectangle or there exists a site not belonging to them at distance one from both. Given a finite set $I \subset \mathbb{Z}^2$, the *bootstrap construction* associates to I a collection of not interacting rectangles through the following sequence of operations: (i) partition I in maximal connected subsets. (ii) Consider the family of rectangles obtained by collecting the rectangular envelope of each maximal connected subset of I. (iii) Partition the family of rectangles in maximal sequences of pairwise interacting rectangles. (iv) Consider a new family of rectangles obtained by collecting the rectangular envelope of the union of the rectangles of each of the maximal sequences constructed at point (iii). (v) Repeat the operations (iii) and (iv) until the family of rectangles constructed at point (iv) is made of pairwise not interacting rectangles.

2.2. The Blume–Capel model

Consider the square $\Lambda = \{1, \dots, L\}^2 \subset \mathbb{Z}^2$. Let $\{-1, 0, +1\}$ be the *single spin state space* and $\mathcal{X} := \{-1, 0, +1\}^\Lambda$ be the *configuration* or *state* space. With **−1**, **0**, **+1** we denote the homogeneous configurations in which all the spins are equal to -1, 0, and $+1$, respectively. Let $\eta \in \mathcal{X}$ and $A \subseteq \Lambda$, we denote by η_A the *restricted configuration* of η on the subset A. We say that two configurations σ and η are *communicating*, and we write $\sigma \sim \eta$, if and only if they differ at most for the value of a spin.

The *Hamiltonian* of the model[1] is

$$H(\eta) = \frac{J}{2} \sum_{\substack{i,j \in \Lambda: \\ |i-j|=1}} [\eta(i) - \eta(j)]^2 + J \sum_{i \in \partial^- \Lambda} \sum_{\substack{j \in \mathbb{Z}^2 \setminus \Lambda: \\ |i-j|=1}} [\eta(i)]^2 - \lambda \sum_{i \in \Lambda} [\eta(i)]^2 - h \sum_{i \in \Lambda} \eta(i) \tag{2.1}$$

for any $\eta \in \mathcal{X}$, where $J > 0$ is called the *coupling constant*, $\lambda, h \in \mathbb{R}$ are called *chemical potential* and *magnetic field* respectively. The first term at the right-hand side of (2.1) will be called *internal interaction* term, the second term *boundary interaction* term, and the last two will be called *site* terms. We stress that the second term accounts for the interaction between the spins at the sites of the internal boundary of Λ and the zero external boundary conditions: each site of the internal boundary contributes with one single bond, excepted for the four sites at the corners of Λ, which contributes with two bonds each. We will refer to $H(\eta)$ as the *energy* of the configuration η.

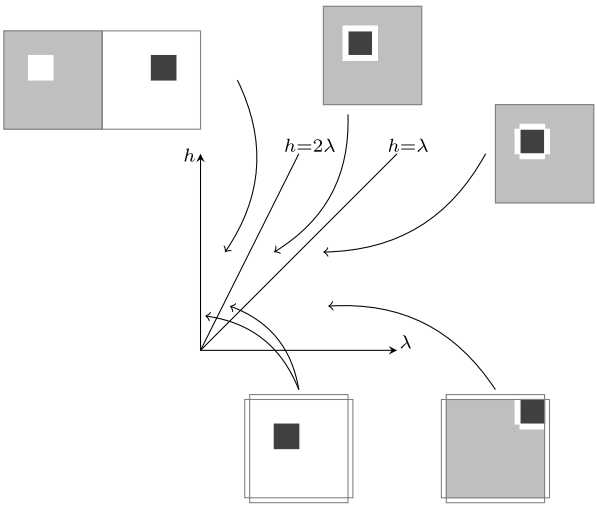

Fig. 1. Schematic representation of the behavior of the Blume–Capel model in the region $h, \lambda > 0$ in the case of periodic boundary condition (top pictures) and in the case of zero-boundary condition (bottom pictures). Gray for minuses, black for pluses, and white for zeros.

In order to state our results we will rely on the following assumptions on the parameters of the model.[2]

Condition 1. *We assume that the parameters of the model satisfy the following properties:*

1. $J \gg \lambda, h > 0$,
2. $L > \left(\frac{2J}{|\lambda - h|}\right)^3$,
3. $\frac{2J}{\lambda+h}$, $\frac{2J}{\lambda-h}$, $\frac{2J+\lambda-h}{\lambda+h}$, $\frac{J+\lambda+h}{h}$ *are not integers.*

Note that the third condition is made so to avoid strong degeneracy of the critical configurations. Similar assumptions are common in literature (see, e.g., [39–41]).

The Gibbs measure associated with the Hamiltonian (2.1) is

$$\mu_\beta(\eta) = \frac{1}{Z_\beta} \exp\{-\beta H(\eta)\}, \tag{2.2}$$

where $Z_\beta = \sum_{\eta' \in \mathcal{X}} \exp\{-\beta H(\eta')\}$ is the *partition function* and $\beta > 0$ the inverse *temperature*.

The time evolution of the model will be defined by assuming that spins evolve according to a Glauber dynamics, with the Metropolis weights. More precisely, we consider the discrete time Markov chain $\sigma_t \in \mathcal{X}$, with $t \geq 0$, with transition matrix p_β defined as follows: $p_\beta(\eta, \eta') = 0$ for $\eta, \eta' \in \mathcal{X}$ not communicating configurations,

$$p_\beta(\eta, \eta') = \frac{1}{2|\Lambda|} e^{-\beta[H(\eta') - H(\eta)]_+} \tag{2.3}$$

for $\eta, \eta' \in \mathcal{X}$ communicating configuration such that $\eta \neq \eta'$ (where, for any real a, we let $[a]_+ = a$ if $a > 0$ and 0 if $a < 0$), and

$$p_\beta(\eta, \eta) = 1 - \sum_{\eta' \neq \eta} p_\beta(\eta, \eta') \tag{2.4}$$

for any $\eta \in \mathcal{X}$. The dynamics can be described as follows: at each time a site is chosen with uniform probability $1/|\Lambda|$ and a spin value differing from the one at the chosen site is selected with probability $1/2$, then the

[1] As mentioned in the Introduction, the Blume–Capel model has several physical applications. In this context its Hamiltonian is usually written in a slightly different way. For instance, in the case of periodic boundary conditions, following [16], we could write

$$\bar{H}(\eta) = -\bar{J} \sum_{\langle i,j \rangle} \eta(i)\eta(j) + \bar{\lambda} \sum_{i \in \Lambda} [\eta(i)]^2 - \bar{h} \sum_{i \in \Lambda} \eta(i),$$

where the sum in the interaction term is extend to the $2|\Lambda|$ not oriented pairs of nearest neighbors. Now, starting from the periodic boundary condition version of the hamiltonian (2.1), namely,

$$H(\eta) = -J \sum_{\langle i,j \rangle} [\eta(i) - \eta(j)] - \lambda \sum_{i \in \Lambda} [\eta(i)]^2 - h \sum_{i \in \Lambda} \eta(i),$$

a straightforward computation yields

$$H(\eta) = -2J \sum_{\langle i,j \rangle} \eta(i)\eta(j) - (\lambda - 4J) \sum_{i \in \Lambda} [\eta(i)]^2 - h \sum_{i \in \Lambda} \eta(i).$$

Thus, the two functions H and $\bar{H}$ coincide provided $\bar{J} = 2J$, $\bar{\lambda} = -(\lambda - 4J)$, and $\bar{h} = h$.

[2] With the notation $0 < a \ll b$ we mean $0 < a < cb$ for some positive constant $c > 1$ that we are not interested to compute exactly.

Table 2.1
Energy difference for a spin flip for all neighbor configurations (opposite sign for reversed flip). The number of neighbor minuses, zeros, and pluses is reported in the first three columns and the energy difference in the last three. For flips at the boundary (resp. corners) see the rows with at least one (resp. two) zero among the nearest neighbors.

Minuses	Zeroes	Pluses	Minus to zero	Minus to plus	Zero to plus
4	0	0	$4J+\lambda-h$	$16J-2h$	$12J-\lambda-h$
3	1	0	$2J+\lambda-h$	$12J-2h$	$10J-\lambda-h$
3	0	1	$+\lambda-h$	$8J-2h$	$8J-\lambda-h$
2	2	0	$+\lambda-h$	$8J-2h$	$8J-\lambda-h$
2	1	1	$-2J+\lambda-h$	$4J-2h$	$6J-\lambda-h$
2	0	2	$-4J+\lambda-h$	$-2h$	$4J-\lambda-h$
1	3	0	$-2J+\lambda-h$	$4J-2h$	$6J-\lambda-h$
1	2	1	$-4J+\lambda-h$	$-2h$	$4J-\lambda-h$
1	1	2	$-6J+\lambda-h$	$-4J-2h$	$2J-\lambda-h$
1	0	3	$-8J+\lambda-h$	$-8J-2h$	$-\lambda-h$
0	4	0	$-4J+\lambda-h$	$-2h$	$4J-\lambda-h$
0	3	1	$-6J+\lambda-h$	$-4J-2h$	$2J-\lambda-h$
0	2	2	$-8J+\lambda-h$	$-8J-2h$	$-\lambda-h$
0	1	3	$-10J+\lambda-h$	$-12J-2h$	$-2J-\lambda-h$
0	0	4	$-12J+\lambda-h$	$-16J-2h$	$-4J-\lambda-h$

flip of the spin at the chosen site to the selected spin value is performed with the Metropolis probability.

The probability measure induced by the Markov chain started at η is denoted by P_η.

Lemma 2.1. *The Markov chain defined above is reversible with respect to the Gibbs measure (2.2), i.e., the detailed balance condition*

$$\mu_\beta(\eta)p_\beta(\eta,\eta') = \mu_\beta(\eta')p_\beta(\eta',\eta) \tag{2.5}$$

is satisfied for any $\eta,\eta' \in \mathcal{X}$.

2.3. Energy landscape

A crucial ingredient for several results discussed in this section and in the following ones is the value of the energy difference (*energy cost*) associated with each possible spin flip.

The energy differences for a spin flip for all neighbor configurations obtained from (2.1) are listed in Table 2.1. Since, as noted above, the boundary interaction term is equal to the internal interaction with fixed zero condition in the external boundary, the energy difference associated with possible spin flips at the boundary is given by the rows of Table 2.1 with at least one zero among the nearest neighbors (at least two for the flip of a spin at the corners of Λ).

As we will see below, the homogeneous states **−1**, **0**, and **+1** will play a crucial role in our study. We remark that, from (2.1), it follows

$$H(\pm\mathbf{1}) = 4JL - |\Lambda|(\lambda \pm h) \text{ and } H(\mathbf{0}) = 0. \tag{2.6}$$

Thus, under the assumptions 1 and 2, the energy hierarchy of the homogeneous states is

$$H(\mathbf{+1}) < H(\mathbf{0}) < H(\mathbf{-1}) \quad \text{for } h \geq \lambda \tag{2.7}$$

and

$$H(\mathbf{+1}) < H(\mathbf{-1}) < H(\mathbf{0}) \quad \text{for } h < \lambda. \tag{2.8}$$

The *ground states* of the system (or of the Hamiltonian) are the configurations where the Hamiltonian (2.1) attains its absolute minimum. We let $\mathcal{X}^s$ be the set of ground states (see, e.g., Fig. 2 for the ground states in the period boundary condition case).

Lemma 2.2. *Under Condition 1 the homogeneous state **+1** is the sole ground state of the system,*[3] *namely, $\mathcal{X}^s = \{\mathbf{+1}\}$.*

[3] We note that if the second term at the right-hand side of (2.1) was not present, then, both for free and periodic boundary conditions, for $\lambda > 0$, the ground state would be the plus homogeneous configuration **+1** for $h > 0$ and the minus homogeneous configuration **−1** for $h < 0$. This would follow from the fact that in these homogeneous states the interaction contribution to the Hamiltonian is zero and the site contribution is minimal.

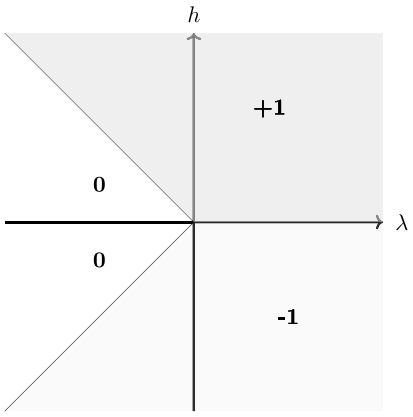

Fig. 2. The zero-temperature phase diagram in the plane $\lambda-h$ in the periodic boundary condition case. The three states **0**, **−1**, **+1** coexist at the point $(0,0)$.

We say that a configuration $\eta \in \mathcal{X}$ is a *local minimum* of the Hamiltonian if and only if for any $\eta' \neq \eta$ communicating with η we have $H(\eta') > H(\eta)$. Important examples of local minima, in suitable regions of the parameter plane $\lambda - h$, are the homogeneous states. We make this remark rigorous in the following lemma.

Lemma 2.3. *Assume 1 is satisfied. For $h > \lambda$ the homogeneous state **0** is a local minimum of the Hamiltonian. For $h < \lambda$ the homogeneous states **0** and **−1** are local minima of the Hamiltonian.*

We stress that for $h > \lambda$ the state **−1** is not a local minimum, indeed, from row 1 in Table 2.1, it follows that the four corner spins can be flipped to zero by decreasing the energy. Moreover, by repeating similar flips a downhill path from **−1** to **0** can be constructed.

2.4. Paths, energy costs, metastable states

A sequence of configurations $(\omega_1,\omega_2,\dots,\omega_n) \in \mathcal{X}^n$ such that ω_i and ω_{i+1} are communicating for any $i = 1,2,\dots,n-1$ is called a *path of length n*. A path $(\omega_1,\dots,\omega_n)$ is called *downhill* (resp. *uphill*) if and only if $H(\omega_i) \geq H(\omega_{i+1})$ (resp. $H(\omega_i) \leq H(\omega_{i+1})$) for any $i = 1,2,\dots,n-1$. In addition, a path $(\omega_1,\dots,\omega_n)$ is called *two-steps downhill* if and only if $H(\omega_i) \geq H(\omega_{i+2}) \geq H(\omega_{i+1})$ for any $i = 1,2,\dots,n-2$. Given two configurations $\eta,\eta' \in \mathcal{X}$, the set of paths with first configuration η and last configurations η' is denoted by $\Omega(\eta,\eta')$.

Given a path $\underline{\omega} = (\omega_1,\dots,\omega_n)$, its *height* $\Phi(\underline{\omega})$ is the maximal energy reached by the configurations of the path, more precisely,

$$\Phi(\underline{\omega}) = \max_{i=1,\dots,n} H(\omega_i)\,. \tag{2.9}$$

Given two configurations η,η', the *communication height* between η and η' is defined as

$$\Phi(\eta,\eta') = \min_{\omega\in\Omega(\eta,\eta')} \Phi(\omega)\,. \tag{2.10}$$

Any path $\omega \in \Omega(\eta,\eta')$ such that $\Phi(\omega) = \Phi(\eta,\eta')$ is called *optimal* for η and η'.

The *stability level* of a configuration $\eta \in \mathcal{X} \setminus \mathcal{X}^s$ is defined as

$$V_\eta := \Phi(\sigma,\mathcal{I}_\eta) - H(\eta), \tag{2.11}$$

where $\mathcal{I}_\sigma$ is the set of configurations with energy strictly lower than $H(\eta)$. The *maximal stability level* is defined as

$$\Gamma_{\rm m} := \max_{\sigma\in\mathcal{X}\setminus\mathcal{X}^{\rm s}} V_\sigma. \tag{2.12}$$

The *metastable states* are defined as the states, different from the ground states, such that their stability level is maximum, namely, it is equal to $\Gamma_{\rm m}$.

Based on Lemma 2.3, at the heuristic level, we can expect that the homogeneous states **−1** and **0** are potential metastable states in the region of the parameter plane considered in the lemma.

3. Main results

In this section, we present the main results of the model.

Beforehand, in Section 3.1 we describe the general metastable behavior in the whole region $0 < h, \lambda \ll J$ using some heuristic arguments. Therefore, in Section 3.2 we state the main results rigorously in the parameter region $\lambda > h > \lambda/2$. Proofs are postponed to Section 4.

3.1. Heuristic discussion

We approach the heuristic study of the Blume–Capel model with zero-boundary conditions in the whole region $0 < h, \lambda \ll J$. We will have to distinguish several subregions where the metastable behavior will show peculiar features.

This analysis is based on a very simple idea: the homogeneous states, if local minima of the Hamiltonian, are potential metastable states of the system. When several possible metastable states are present, the true one is the one from which the system has to overcome the largest barrier to reach the stable state. In order to compute such a barrier we imagine that the transition is realized through a sequence of local minima in which a droplet of stable phase grows in the sea of the metastable one.

3.1.1. Region $h > \lambda > 0$

In view of Lemma 2.3 we are interested in the structures that give rise to local minima with zero background.

From rows 13–15 of Table 2.1 it follows that a configuration in which the sites with plus spin form a rectangle plunged in the sea of zeros is a local minimum. We stress that the rectangular plus droplet can be located at one corner of the lattice Λ. We add that if the shape of the plus region is not a rectangle, then, since there exists at least a zero with more than two neighboring pluses, from rows 13–15 of Tables 2.1 it follows that the configuration is not a local minimum.

The energy of a square plus droplet of side length ℓ plunged in the sea of zeros with respect to the energy of **0** is $4JL - (\lambda + h)\ell^2$. Since its maximum is attained at $2J/(\lambda + h)$, we can infer that this is the critical length, in the sense that droplets with side length smaller than $2J/(\lambda + h)$ tend to shrink, otherwise they tend to grow. Moreover, we note that the difference of energy between the critical droplet and the configuration **0** is $4J^2/(\lambda + h)$.

At the level of our very rough heuristic discussion, we can conclude that the metastable state is the **0** configuration, the transition to the stable state is performed via the nucleation of a square droplet of pluses of side length $2J/(\lambda + h)$ at any site of the lattice Λ (homogeneous nucleation), and the exit time is of order $\exp\{\beta 4J^2/(\lambda + h)\}$.

3.1.2. Region $\lambda > h > 0$

In view of Lemma 2.3 we are interested in the structures that give rise to local minima with zero or minus background.

In the case of zero background, the same discussion as in Section 3.1.1 suggests that the system can exit the state **0** by overcoming the energy barrier $4J^2/(\lambda + h)$ and reaching the stable state **+1** via the formation of a critical square droplet of pluses with side length $2J/(\lambda+h)$. But also the possibility that the system abandons **0** reaching **−1** must be explored: from rows 1, 2, and 4 of Table 2.1 it follows that a configuration in which the sites with minus spin form a rectangle plunged in the sea of zeros is a local minimum. The energy of a square minus droplet of side length ℓ plunged in the sea of zeros with respect to the energy of **0** is $4JL - (\lambda - h)\ell^2$. The critical length is $2J/(\lambda - h)$ and the difference of energy between the critical droplet and the configuration **0** is $4J^2/(\lambda - h)$. Since in this parameter region $4J^2/(\lambda + h) < 4J^2/(\lambda - h)$ we can conclude that the system, starting from **0**, will perform a direct transition to the stable state **+1** paying the energy cost $4J^2/(\lambda + h)$.

For what concerns the minus background case, we note[4] that a rectangle of pluses in the sea of minuses is not a local minimum, since (see row 6 of Table 2.1) the flip to zero of one plus with two pluses and two minuses among its neighbors (corner) decreases the energy of the configuration.

Some relevant structures that are local minima are reported in Fig. 3. To prove that the depicted structures are local minima the reader can use Table 2.1. The five structures in the figure will be addressed in the sequel as (a) *frame*, (b) *boundary frame*, (c) *corner frame*, (d) *chopped corner frame*, (e) *chopped boundary frame*.

For each structure we compute its energy with respect to **−1** as a function of the side length ℓ of the internal plus square. With an intuitive notation we have:

$$\begin{aligned}
\Delta_{\rm a}(\ell) &= -2h\ell^2 + 4J\ell + 4J(\ell+2) + 4\ell(\lambda - h),\\
\Delta_{\rm b}(\ell) &= -2h\ell^2 + 4J\ell + 2J(\ell+2) + (4\ell+2)(\lambda - h),\\
\Delta_{\rm c}(\ell) &= -2h\ell^2 + 4J\ell + (4\ell+3)(\lambda - h),\\
\Delta_{\rm d}(\ell) &= -2h\ell^2 + 2J\ell + 2J(\ell+1) - 2J + 2\ell(\lambda - h),\\
\Delta_{\rm e}(\ell) &= -2h\ell^2 + 3J\ell + J(3\ell+2) + 3\ell(\lambda - h).
\end{aligned} \tag{3.13}$$

Now, we note that

$$\begin{aligned}
\Delta_{\rm a} - \Delta_{\rm d} &= 4J\ell + 8J + 2\ell(\lambda - h),\\
\Delta_{\rm b} - \Delta_{\rm d} &= 2J\ell + 4J + (2\ell+2)(\lambda - h),\\
\Delta_{\rm c} - \Delta_{\rm d} &= (2\ell+3)(\lambda - h),\\
\Delta_{\rm e} - \Delta_{\rm d} &= 2J\ell + 2J + \ell(\lambda - h).
\end{aligned} \tag{3.14}$$

Since these differences are all positive, we can conclude that the mechanism providing the transition from **−1** to **+1** is the formation and growth of a chopped corner droplet.

The length ℓ maximizing the energy (critical length) of such droplet is $[2J + (\lambda - h)]/(2h)$ and the energy of the critical droplet, with respect to **−1**, in the limit $0 < h < \lambda \sim 0$ is $2J^2/h$.

At the level of this heuristic analysis, it seems that the mechanism of the chopped corner frame is the best to perform the transition from the homogeneous **−1** state to the stable state **+1**. This transition is performed via the nucleation of a chopped corner frame of internal side length $[2J + (\lambda - h)]/(2h)$ (not homogeneous nucleation) and the exit time is of order $\exp\{\beta 2J^2/h\}$. To establish which, between **−1** and **0**, is the metastable state in the region $0 < h < \lambda$ we note that in this region of the parameter plane $4J^2/(\lambda + h) < 2J^2/h$ and, so, the metastable state is **−1**. Moreover, we remark some relevant facts: the transition from the metastable to the stable state is direct (i.e., not mediated by an intermediate phase), the nucleation is not homogeneous, and the exit time does not depend on λ.

[4] We also note that a rectangle of zeros in the sea of minuses is not a local minimum, since (see row 4 of Table 2.1) the flip to minus of one zero with two zeros and two minuses among its neighbors (corner) decreases the energy of the configuration. But this remark is not relevant from the metastability point of view, since, in view of (2.8), the transition from **−1** to **0** is of no interest in this region of the parameters.

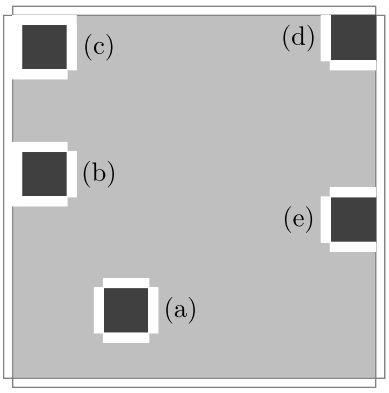

Fig. 3. Representation of local minima in the sea of minuses. Light gray for minuses, black for pluses, and white for zeros.

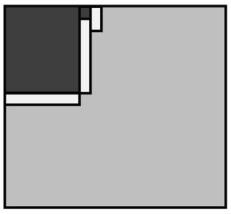

σ_s

Fig. 4. The critical configuration σ_s. Black, white, and gray sites represent pluses, zeros, and minuses respectively. The rectangle of pluses has side lengths l_c and $l_c - 1$.

3.2. Main results for the region $\lambda > h > \lambda/2$

We note that the condition $h > \lambda/2$ is purely technical and useful to keep simple the argument used in the proofs, indeed our findings should be valid in the whole region $\lambda > h > 0$ as suggested by the heuristic discussion of Section 3.1.

The first theorem states that every configuration of $\mathcal{X}$ different from $\{-\mathbf{1}, +\mathbf{1}\}$ has a stability level strictly

smaller than

$$\Gamma := H(\sigma_s) - H(-\mathbf{1}) = 4Jl_c + 2\lambda l_c - 2hl_c^2 - 2h, \tag{3.15}$$

where

$$l_c = \lfloor \frac{2J + \lambda - h}{2h} \rfloor + 1, \tag{3.16}$$

and σ_s is the critical configuration represented in Fig. 4.

Proposition 3.1. *Let $\eta \in \mathcal{X}$ be a configuration such that $\eta \notin \{-\mathbf{1}, +\mathbf{1}\}$, then $V_\eta < \Gamma$.*

This result suggests that the only configurations with a stability level greater than or equal to Γ could be $-\mathbf{1}$ and $+\mathbf{1}$. This is confirmed by Theorem 3.1, where we identify the unique metastable state $-\mathbf{1}$ and the stable state $+\mathbf{1}$ in the region $\lambda > h > 0$, and we compute the maximal stability level.

Theorem 3.1 (*Identification of the Metastable State*). *In the region $\lambda > h > \lambda/2$, the unique metastable state is $-\mathbf{1}$ and $\Gamma_m = \Gamma$.*

In the following theorem, we state the recurrence of the system to the set $\{-\mathbf{1}, +\mathbf{1}\}$. In particular, (3.18) implies that the system reaches with high probability either the state $-\mathbf{1}$ (which is a local minimizer of the Hamiltonian) or the ground state in a time shorter than $e^{\beta(\Gamma+\epsilon)}$, uniformly in the starting configuration η for any $\epsilon > 0$. In other words we can say that the dynamics speeded up by a time factor of order $e^{\beta\Gamma}$ reaches with high probability $\{-\mathbf{1}, +\mathbf{1}\}$. To make this statement rigorous, for the chain σ_t started at $\eta \in \mathcal{X}$, we define the *first hitting time* from $\eta \notin \mathcal{Y}$ to $\mathcal{Y} \subset \mathcal{X}$ in the following way

$$\tau_{\mathcal{Y}} := \inf_{t>0}\{t : \sigma_t \in \mathcal{Y}\}. \tag{3.17}$$

Theorem 3.2 (*Recurrence Property*). *For any $\epsilon > 0$ and sufficiently large β, the function*

$$\beta \to \sup_{\eta\in\mathcal{X}} \mathbb{P}_\eta(\tau_{\{-\mathbf{1},+\mathbf{1}\}} > e^{\beta(\Gamma+\epsilon)}) \tag{3.18}$$

is super-exponentially small.[5]

The last goal is that of finding the asymptotic behavior as $\beta \to \infty$ of the transition time for the system started at the metastable state $-\mathbf{1}$.

Theorem 3.3 (*Asymptotic Behavior of $\tau_{+\mathbf{1}}$ in Probability*). *For any $\epsilon > 0$, we have*

$$\lim_{\beta\to\infty} \mathbb{P}_{-\mathbf{1}}(e^{\beta(\Gamma-\epsilon)} < \tau_{+\mathbf{1}} < e^{\beta(\Gamma+\epsilon)}) = 1. \tag{3.19}$$

4. Proof of the main results

In this section we collect the proofs of the lemmas of Section 2 and the theorems of Section 3.

4.1. Proof of Lemma 2.1

The statement is trivial in the cases η and η' not communicating and $\eta' = \eta$. Thus, suppose $\eta \neq \eta'$ are communicating: if $H(\eta) = H(\eta')$ then (2.5) is immediate, on the other hand if $H(\eta') > H(\eta)$ (the opposite case can be treated analogously) the statements follows from the definition of the Gibbs measure (2.2) and the fact that

$$p_\beta(\eta, \eta') = \frac{1}{2|\Lambda|} e^{-\beta[H(\eta')-H(\eta)]} \text{ and } p_\beta(\eta', \eta) = \frac{1}{2|\Lambda|}. \quad \square$$

4.2. Proof of Lemma 2.2

Recall we assumed that Condition 1 is in force.

Case 1: pick a configuration $\eta \neq +\mathbf{1}$, such that there is at least one minus spin. Consider the configuration η' obtained by flipping in η all the minuses to plus. We claim that $H(\eta') < H(\eta)$, indeed, (i) the internal interaction term at the right-hand side of (2.1) is smaller for η' since nothing changes for the bonds between minus spins of η and for the bonds in which, in η, one site has spin minus and the other has spin zero, on the other hand the interaction decreases if, in η, one of the sites of the bond has spin minus and the other has spin plus; (ii) the boundary interaction term is the same in η and η'; (iii) the chemical potential term in η' is the same as the one in η; (iv) the magnetic field in η' is smaller than that in η by the amount $2h$ for each flipped spin. If $\eta' = +\mathbf{1}$ the proof is over, otherwise there exists in η' at least one zero spin and the proof will be completed in the following case.

Case 2: consider a configuration $\eta' \neq +\mathbf{1}$, such that there is no minus spin. Consider the configuration η'' obtained by flipping to plus all the zero spins in η' associated with the sites belonging to one of the not interacting rectangles obtained by applying the bootstrap construction (see Section 2.1) to the set of sites where η' is plus one. If $\eta'' \neq \eta'$ then $H(\eta'') < H(\eta')$ because it is possible to construct a downhill path from η' to η'' such that at each step a zero spin with at least two neighboring plus sites and no neighboring minus is flipped to plus decreasing the energy of the configurations (see rows 13–15 in Table 2.1). If $\eta'' = +\mathbf{1}$ the proof is over. In case $\eta'' \neq +\mathbf{1}$, let ℓ be the largest side length of the rectangles in which η'' is plus one and consider the following cases.

[5] We say that a function $\beta \mapsto f(\beta)$ is super exponentially small if $\lim_{\beta\to\infty} \frac{\log f(\beta)}{\beta} = -\infty$.

Case 2.1: suppose $\ell < 2J/(h+\lambda)$. Consider the configuration η''' obtained by flipping to zero all the pluses in one of the sides of length ℓ. From (2.1) we get $H(\eta''') - H(\eta'') = -2J + (\lambda+h)\ell$, which implies $H(\eta''') < H(\eta'')$. By removing one side after the other we prove $H(\mathbf{0}) < H(\eta')$ and, from (2.7), which is valid under the hypotheses of this lemma, we get $H(\mathbf{+1}) < H(\eta')$.

Case 2.2: suppose $\ell > 2J/(h+\lambda)$. Now, consider one of the rectangles on which η'' is plus one with maximal side length equal to ℓ. Consider the configuration η'''' obtained by flipping to plus all the zeros associated with sites neighboring one of the sides of this rectangle whose length is equal to ℓ. From (2.1) we get $H(\eta'''') - H(\eta'') = 2J - (\lambda+h)\ell$, which implies $H(\eta'''') < H(\eta'')$.

If η'' has a single rectangle of pluses, this growth mechanism can be continued until $\mathbf{+1}$ is obtained proving the statement of the lemma. If η'' has two or more rectangles of pluses, this growth mechanism can be continued until two or more interacting rectangles are found. In such a case, by performing bootstrap mechanism steps and boundary growth of rectangles the $\mathbf{+1}$ configuration will be eventually constructed completing the proof of the lemma. □

4.3. Proof of Lemma 2.3

Case $h > \lambda$: row 11 of Table 2.1 implies that the state $\mathbf{0}$ is a local minimum of the Hamiltonian, since all the possible spin flips have a positive energy cost.

Case $h < \lambda$: the fact that $\mathbf{0}$ is a local minimum is proven as above. Moreover, from row 1 of the Tables 2.1 it follows that the state $\mathbf{-1}$ is a local minimum of the Hamiltonian, as well. □

4.4. Proof of Proposition 3.1

The proof of Proposition 3.1 is based on Lemmas. 4.4–4.10. which are listed at the end of this subsection. We prove that for every configuration $\eta \notin \{\mathbf{-1},\mathbf{+1}\}$, the stability level is strictly smaller than the energy barrier Γ.

First of all, given a configuration $\eta \in \mathcal{X}$, we consider the set $C(\eta) \subseteq \mathbb{R}^2$ defined as the union of the closed unitary square centered at sites i with the boundary parallel to the axes of $\mathbb{Z}^2$ and such that $\eta(i) = +1$.

The maximal connected components $C_1, \dots, C_m$, with $m \in \mathbb{N}$, of $C(\eta)$ are called *clusters of pluses*. We define in the same way the *clusters of minuses* and the *clusters of zeros*. The boundary of each cluster is made of straight lines and corners, that can be *convex corners* or *concave corners* following the usual $\mathbb{R}^2$ definitions. Moreover, the straight portion of the boundary delimited by two subsequent convex corners is called a *convex side* of the boundary, otherwise it is called a *concave side*.

We observe that each cluster has at least one convex side, since Λ is finite and we have assumed zero-boundary conditions.

In order to prove Proposition 3.1, in the following lemmas, we partition the set of all configurations in suitable families according to peculiar properties of their clusters and we provide their stability levels, that turn out to be strictly smaller than Γ. In particular, we first analyze the configurations with at least a cluster of pluses, see Lemmas 4.4, 4.5, 4.6, 4.7, 4.8, 4.9. In addition, in Lemmas 4.6, 4.7, and 4.10 we discuss the configurations containing only zero and minus spins. The proofs of the previous lemmas are reported in Appendix A.1. □

Lemma 4.4. *If η is a configuration that contains a bond with minus and plus spins, then there exists a configuration η' such that $H(\eta') < H(\eta)$ and the two configurations communicate with a downhill path.*

Lemma 4.5. *If η is a configuration that contains at least a cluster of pluses which is not a rectangle in $\mathbb{R}^2$, then $V_\eta < 2(\lambda - h)$.*

Lemma 4.6. *If η is a configuration that contains either a cluster of pluses which is a rectangle of $\mathbb{R}^2$ with one side length $l_1 < \frac{2J}{\lambda+h}$ or a cluster of minuses with at least a convex side with length $l_2 < \frac{2J}{\lambda-h}$, then $V_\eta < 2J$.*

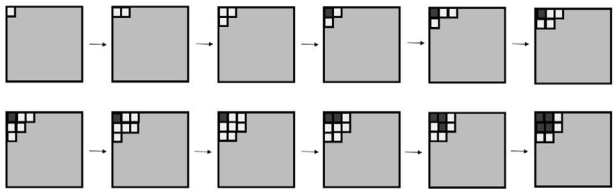

Fig. 5. The first part of the reference path, from $\mathbf{-1}$ to $\sigma^F_{2,2}$, a chopped corner frame of both side lengths equal to two.

Lemma 4.7. *If η is a configuration that contains a cluster of pluses (resp. a cluster of minuses) which is a rectangle of $\mathbb{R}^2$ with at least one side length $l_1 > \frac{2J}{\lambda+h}$ (resp. $l_2 > \frac{2J}{\lambda-h}$) at distance strictly greater than two from a minus (resp. plus) spin, then $V_\eta < 2J$.*

Lemma 4.8. *If η is a configuration that contains a cluster of pluses which is a rectangle of $\mathbb{R}^2$ with at least one side length $l > \frac{2J+\lambda-h}{h}$, then $V_\eta < 5J$.*

Lemma 4.9. *If η is a configuration that contains a cluster of pluses which is a rectangle of $\mathbb{R}^2$ with at least one side length $\frac{2J}{\lambda+h} < l < \frac{2J+\lambda-h}{h}$, then we have $V_\eta < \Gamma$.*

Lemma 4.10. *The stability level of $\mathbf{0}$ is strictly smaller than Γ, i.e., $V_{\mathbf{0}} < \Gamma$.*

4.5. Proof of Theorem 3.1

To prove the theorem we have to identify the unique metastable state and compute the value of the maximal stability level.

In order to do this, we first construct in Section 4.5.1 a reference path to find an upper bound to the communication height between $\mathbf{-1}$ and $\mathbf{+1}$ and then, in Section 4.5.2, we prove a lower bound by using a new strategy based on the computation of the number of bonds in any configuration. More precisely, we shall first prove $\Phi(\mathbf{-1},\mathbf{+1}) - H(\mathbf{-1}) \le \Gamma$ and then $\Phi(\mathbf{-1},\mathbf{+1}) - H(\mathbf{-1}) \ge \Gamma$.

These results and Proposition 3.1 above, together with [9, Theorem 2.2] yield the theorem. □

4.5.1. Upper bound to $\Phi(\mathbf{-1},\mathbf{+1}) - H(\mathbf{-1})$

We define the *reference path* ω^r as a path from $\mathbf{-1} \to \mathbf{+1}$ consisting in a sequence of configurations with increasing clusters *as close as possible to chopped corner frame* such that $\Phi(\omega^r) - H(\mathbf{-1}) = \Gamma$. This implies that

$$\Phi(\mathbf{-1},\mathbf{+1}) - H(\mathbf{-1}) \le \Gamma. \tag{4.20}$$

We denote by $\sigma_{m,n}$ the configuration that contains a chopped corner frame such that the rectangle of pluses has horizontal and vertical side length equal to m and n.

In order to construct the path, see Fig. 5, we start by choosing one of the four corners of Λ and we consider its two nearest neighbors. We flip, one after the other in any order, these two minus spins to zero with the energy cost that is independent on the order and equal to $3(\lambda - h)$, see Table 2.1. Then, we flip the zero in the corner to plus increasing the energy by $4J - (\lambda + h)$. Thus the total energy cost to construct $\sigma_{1,1}$, i.e. to form a chopped corner frame of both side lengths equal to one, is $4J + 2\lambda - 4h$.

Next, we first flip to zero the minus spins at distance smaller than or equal to $\sqrt{2}$ from the zeros of $\sigma_{1,1}$ starting from those closest and then we construct a 2×2 square of pluses. In this way a chopped corner frame of both side lengths two is formed, see Fig. 5.

We grow up this chopped corner frame by applying the following steps: (i) flipping to zero with the energy cost $\lambda - h$ a minus spin at distance one from this frame and from the boundary of Λ (this is the effect of the zero-boundary conditions); (ii) flipping to plus the unique

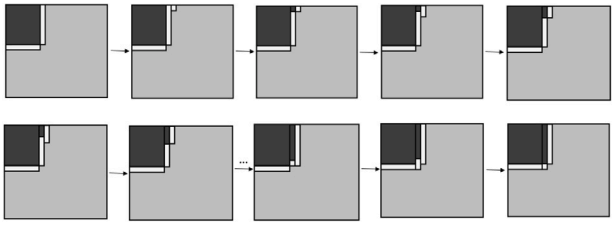

Fig. 6. A part of the reference path from $\sigma_{n-1,n}$ to $\sigma_{n,n}$.

zero with two zero nearest neighbors; (iii) repeating steps (i) and (ii) to grow up the chopped corner frame 2×2 to a chopped corner frame 2×3, namely, $\sigma_{2,3}$. Next, we grow up the chopped corner frame 2×3 by performing similar steps along its longest side and obtaining $\sigma_{3,3}$.

This growth mechanism can be iterated, always by flipping first a minus to zero and then a zero to plus, see Figure 6, until the chopped corner frame invades all the lattice Λ and the configuration $\mathbf{+1}$ is reached.

In order to compute the height of this path, we first evaluate the height of the portion of the path connecting $\mathbf{-1}$ to a general configuration $\sigma_{m,n}$. Suppose $m\le n$, we have

$$H(\sigma_{m,n}) = 2J(n+m) + 4JL - (\lambda+h)nm - (\lambda-h)(L^2 - nm - n - m), \tag{4.21}$$

where $2(m+n)$ is the number of bonds with spins 0 and $+1$, $4L$ is the number of bonds with spins 0 and -1, mn is the number of pluses, and $(L^2-nm-n-m)$ is the number of minuses in $\sigma_{m,n}$. Thus, by (2.6), we get

$$H(\sigma_{m,n}) - H(\mathbf{-1}) = 2J(n+m) + \lambda(n+m) - h(2mn+n+m) \tag{4.22}$$

By using (4.22) one can compute explicitly $H(\sigma_{n,n-1})$, $H(\sigma_{n,n})$, and $H(\sigma_{n,n+1})$ and prove that

$$H(\sigma_{n,n-1}) \gtrless H(\sigma_{n,n}) \gtrless H(\sigma_{n,n+1}) \text{ if } n \gtrless \frac{2J+\lambda-h}{2h}.$$

Thus, the height of the reference path $\Phi(\omega^{\mathrm{r}})$ is equal to $\Phi(\sigma_{l_c,l_c-1},\sigma_{l_c,l_c})$, where l_c is defined in (3.16).

The maximal energy reached by the portion of the path from σ_{l_c,l_c-1} to σ_{l_c,l_c} is achieved after the first three steps and its value is $2J-(\lambda+h)+2(\lambda-h)$. Indeed, the first step is the flip to zero of the minus spin at distance one from the chopped corner frame and from the boundary of Λ, which costs $\lambda-h$. The second step is the flip to plus of the unique zero with two zero nearest neighbors which costs $2J-(\lambda+h)$. The third step is the flip to zero of the minus at distance one from the first flipped minus and two from the boundary of Λ, which costs $\lambda-h$. The remaining part of the considered portion of the path yielding to σ_{l_c,l_c} is a sequence of flips of zeros to plus with the energy decrease $\lambda+h$ followed by flips of minuses to zero with energy cost $\lambda-h$, which implies that this portion of the path is a two-steps downhill path.

Finally, by (4.22), we have

$$\begin{aligned}\Phi(\mathbf{-1},\mathbf{+1}) - H(\mathbf{-1}) &\le \Phi(\omega^{\mathrm{r}}) - H(\mathbf{-1})\\ &= \Phi(\sigma_{l_c,l_c-1},\sigma_{l_c,l_c}) - H(\mathbf{-1})\\ &= H(\sigma_{l_c,l_c-1}) + 2J - (\lambda+h) + 2(\lambda-h) - H(\mathbf{-1})\\ &= 4Jl_c + 2\lambda l_c - 2hl_c^2 - 2h = \Gamma,\end{aligned} \tag{4.23}$$

which proves (4.20).

4.5.2. Lower bound to $\Phi(\mathbf{-1},\mathbf{+1}) - H(\mathbf{-1})$

We use the Lemmas. 4.11–4.18, which are collected at the end of this subsection, to prove the lower bound

$$\Phi(\mathbf{-1},\mathbf{+1}) - H(\mathbf{-1}) \ge \Gamma. \tag{4.24}$$

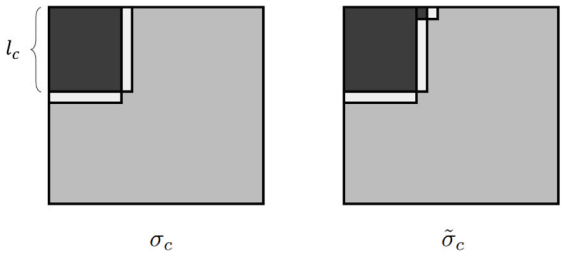

Fig. 7. Configurations σ_c and $\tilde{\sigma}_c$. The cluster of pluses with side lengths l_c and l_c-1, can be in one of the four corners of Λ and the protuberance can be attached along one of the two sides of the rectangular cluster of pluses and near the boundary of Λ. With an abuse of notation, we denote all of these configurations with σ_c and $\tilde{\sigma}_c$.

We denote by $\mathcal{M}_{n^+}$ the set of configurations with n^+ plus spins. We set

$$n_c^+ := l_c(l_c-1) \quad \text{and} \quad \sigma_c = \sigma_{l_c-1,l_c} \in \mathcal{M}_{n_c^+}, \tag{4.25}$$

see Fig. 7. We remark that in σ_c the smallest rectangle that contains the frame of pluses and zeros has side lengths l_c and l_c+1. The envelope of this rectangle contains $2(2l_c-1)$ bonds between a plus and a zero, and $2l_c+1$ bonds between a minus and a zero. The other bonds in the envelope are between two spins of the same type. Outside this envelope there are $4L-(2l_c+1)$ bonds between a minus and a zero according to the zero-boundary conditions, and the other bonds are between two spins of the same type.

Moreover, we introduce the peculiar configurations $\tilde{\sigma}_c$, see Fig. 7, which will play a crucial role in the proof. It is useful to compare $\tilde{\sigma}_c$ and σ_c with the configuration σ_s introduced in Fig. 4.

We remark that the energy of the configurations $\tilde{\sigma}_c$ and σ_s is larger than that of σ_c, indeed,

$$H(\tilde{\sigma}_c) = H(\sigma_c) + 2J - (\lambda+h) + (\lambda-h) \tag{4.26}$$

and

$$H(\sigma_s) = H(\sigma_c) + 2J - (\lambda+h) + 2(\lambda-h). \tag{4.27}$$

We also note that $H(\sigma_s) = H(\tilde{\sigma}_c) + (\lambda-h)$ and that, by Table 2.1, the minimal energy quantum to be paid to jump from $\tilde{\sigma}_c$ to σ_s is $\lambda-h$. This implies that, for any configuration $\eta\in\mathcal{X}$,

$$\text{if } H(\eta) > H(\tilde{\sigma}_c) \text{ then } H(\eta) \ge H(\sigma_s). \tag{4.28}$$

We are now ready to discuss the proof of (4.24) and we split it into two main steps.

First step: we prove that σ_c in (4.25) is the energy minimizer of the manifold $\mathcal{M}_{n_c^+}$, that is $\sigma_c = \operatorname{argmin}_{\xi\in\mathcal{M}_{n_c^+}} H(\xi)$. This is achieved in Lemma 4.14 by means of Lemmas. 4.11–4.13. The strategy of proof implemented by the lemmas is essentially the following: all the configurations in $\mathcal{M}_{n_c^+}$ are taken into account and it is proven that any configuration η differing from σ_c does not belong to the set of minimizers

$$M = \{\sigma \mid H(\sigma) = \min_{\xi\in\mathcal{M}_{n_c^+}} H(\xi)\}. \tag{4.29}$$

Second step: we use the information on the minimum of the energy in the manifold $\mathcal{M}_{n_c^+}$ proven in the first step to get (4.24), by considering all the paths from $\mathbf{-1}$ to $\mathbf{+1}$ and showing that their height is larger than or equal to $H(\sigma_s)$.

Indeed, since all such paths must necessary visit the set $\mathcal{M}_{n_c^+}$, we can partition them in those that do not pass through σ_c and those that visit such configuration. The first ones are treated in Lemma 4.15, while for other ones, namely, those visiting σ_c, we consider the following three alternatives:

(a) the path visits $\tilde{\sigma}_c \in \mathcal{M}_{n_c^+ +1}$, see Lemma 4.16;

(b) the path visits a configuration $\eta \in \mathcal{M}_{n_c^+ +1}$ different from $\tilde{\sigma}_c$ but with the same energy, see Lemmas 4.17 and 4.18;
(c) the path visits a configuration in $\mathcal{M}_{n_c^+ +1}$ with energy strictly larger than $H(\tilde{\sigma}_c)$ and thus the energy is larger than or equal to $H(\sigma_s)$, as observed in (4.28).

The proof of (4.24) is thus concluded.

Lemma 4.11. *If $\eta \in \mathcal{M}_{n_c^+}$ is a configuration that contains at least a column (or a row) with only zero spins, then $\eta \notin M$.*

Lemma 4.12. *Let $\eta \in \mathcal{M}_{n_c^+}$ be a configuration that contains a cluster of pluses with a shape different from a rectangle (a quasi-square) with side lengths l_c and $l_c - 1$. Then $\eta \notin M$.*

Lemma 4.13. *If $\eta \in \operatorname{argmin}_{\xi \in \mathcal{M}_{n_c^+}} H(\xi)$, then the following conditions hold:*

(i) η contains a cluster of pluses which is a rectangle (a quasi-square) of $\mathbb{R}^2$ with side lengths l_c and $l_c - 1$;
(ii) Let Q be the rectangle of sites inside the cluster of pluses, we have $\eta_Q = \mathbf{+1}_Q$, $\eta_{\Lambda \setminus (Q \cup \partial^+ Q)} = \mathbf{-1}_{\Lambda \setminus (Q \cup \partial^+ Q)}$, and $\eta_{\partial^+ Q} = \mathbf{0}_{\partial^+ Q}$,

Lemma 4.14. $H(\sigma_c) = \min_{\xi \in \mathcal{M}_{n_c^+}} H(\xi)$.

Lemma 4.15. *If $\underline{\omega}$ is a path from $\mathcal{M}_{n_c^+} \setminus \{\sigma_c\}$ to $\mathcal{M}_{n_c^+ +1}$, then $\Phi(\underline{\omega}) > H(\tilde{\sigma}_c)$ and, hence, $\Phi(\omega) \geq H(\sigma_s)$.*

Lemma 4.16. *If $\underline{\omega}$ is a path from $\tilde{\sigma}_c$ to $\mathcal{M}_{n_c^+ +2}$ such that $\underline{\omega} = (\tilde{\sigma}_c, \eta_1, \eta_2, \dots \eta_n)$, with $n \geq 1$, $\eta_n \in \mathcal{M}_{n_c^+ +2}$, and $\eta_i \in \mathcal{M}_{n_c^+ +1}$ for every $i = 1, \dots, n-1$, then $\Phi(\underline{\omega}) \geq H(\sigma_s)$.*

Before stating the last lemmas we agree on calling *strip of pluses* (resp. *strip of minuses*) a connected subset of a column or a row of Λ filled with all the spins equal to plus (resp. equal to minus). Moreover, we define the set $\mathcal{S}$ as the set of all configurations of $\mathcal{M}_{n_c^+ +1}$ such that

a. bonds with a spin plus and a spin minus are not present;
b. there exists a single cluster of pluses and its half-perimeter is equal to $2l_c$;
c. the minimal rectangle of $\mathbb{R}^2$ that contains the cluster of pluses has either side lengths (l_c, l_c) or $(l_c + 1, l_c - 1)$;
d. one of the sites lying in the cluster of pluses is one of the four corners of Λ;
e. there is only one strip of minuses in each column and row of Λ.

We note that $\tilde{\sigma}_c \in \mathcal{S}$.

Lemma 4.17. *Let $\eta \in \mathcal{M}_{n_c^+ +1}$ be such that $H(\eta) = H(\tilde{\sigma}_c)$, then $\eta \in \mathcal{S}$.*

Lemma 4.18. *Let $\eta \in \mathcal{S} \setminus \{\tilde{\sigma}_c\}$. Every path $\underline{\omega}$ connecting η to $\mathbf{-1}$ is such that $\Phi(\underline{\omega}) > H(\sigma_s)$.*

The proofs of the previous lemmas are in Appendix A.2.

4.6. Proof of Theorem 3.2

By applying [21, Theorem 3.1] for $V^* = \Gamma$ and Proposition 3.1, we get (3.18). □

4.7. Proof of Theorem 3.3

The results in Theorem 3.1 above, together with [21, Theorem 4.1] with $\eta_0 = \mathbf{-1}$ yield the theorem. □

5. Conclusions and perspectives

We investigated the metastable behavior of the stochastic Blume–Capel model evolving according to the Glauber dynamics with zero-boundary conditions. We have shown that, due to the three-state character of the model, the metastability scenario changes profoundly with respect to the one proven in previous papers where periodic boundary conditions are assumed.

The Hamiltonian of the Blume–Capel model is characterized by the magnetic field h and the chemical potential λ. For $\lambda, h > 0$ the chemical potential term equally favors minus and plus spins with respect to zeros, while the magnetic field favors pluses and penalizes minuses with respect to the zeros. A thorough heuristic study suggested that the region in which the effect of the boundary conditions is more relevant is the sector $\lambda > h > 0$. We thus restricted our rigorous analysis to this part of the parameter space adding the supplementary technical restriction $h > \lambda/2$.

We have proven that the unique metastable state is $\mathbf{-1}$ and we have computed the energy barrier from $\mathbf{-1}$ to the stable state $\mathbf{+1}$, yielding an estimate for the asymptotic behavior of the exit time as $\beta \to \infty$, where β is the inverse temperature. We have also shown that the nucleation is heterogeneous in the sense that it is performed via the appearance of a critical droplet localized in one of the corners of the lattice.

In order to get the energy barrier we have computed an upper bound by means of classical techniques, see [21,22], while to find the lower bound we have provided new ideas and methods based on the partition of the lattice into columns and rows with different interactions inside.

We remark finally, that this paper is part of a long term project having as final goal the study of the metastable behavior of the Blume–Capel model with the (conserved) Kawasaki dynamics. We expect different behaviors at the level of the exit path with respect those proven for the non-conserved dynamics in the present paper. Indeed, it is well known that the exit paths from a metastable state are strongly affected by the details of the considered stochastic dynamics.

In order to implement such a dynamics, indeed, it is necessary to give up the periodic boundary conditions in favor of the zero ones. The results proven in this paper for the Glauber dynamics are thus a necessary first step that will be the starting point of our future investigations.

Moreover, we expect that the techniques and the machinery developed in this paper will be useful in solving the much more intricate problems arising in the Kawasaki setup.

CRediT authorship contribution statement

Emilio N.M. Cirillo: Conceptualization, Methodology. **Vanessa Jacquier:** Conceptualization, Methodology, Writing – original draft, Writing – review & editing. **Cristian Spitoni:** Conceptualization, Methodology.

Declaration of competing interest

The authors declare that they have no known competing financial interests or personal relationships that could have appeared to influence the work reported in this paper.

Data availability

No data was used for the research described in the article.

Acknowledgments

ENMC acknowledges that this work has been done under the framework of GNMF and PRIN 2022 project “Mathematical modelling of heterogeneous systems". VJ thanks GNAMPA (CUP B53D23009360006).

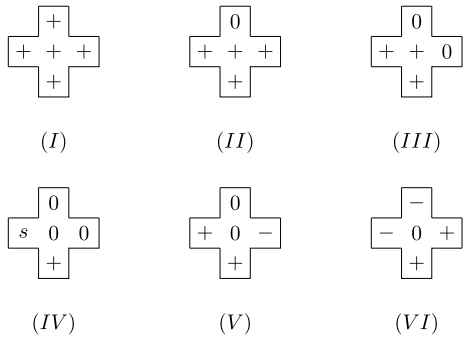

Fig. A.8. Local configurations with at least a plus spin whose energy cannot be decreased via a single spin flip. The spin s in (IV) takes value in $\{-1,0\}$.

Appendix. Proof of lemmas

In this appendix we collect the proofs of the lemmas of Section 4.

A.1. Proofs of lemmas in Section 4.4

Proof of Lemma 4.4. Using Table 2.1, it is possible to reduce the energy of all configurations with a bond with minus and plus spins except the configuration where the plus and the minus have three pluses and three minuses, respectively, as neighboring spins.

In the latter case, we analyze the two columns (or rows) to which the plus and the minus belong to until we possibly find a bond different from $(+,-)$. In such a case the energy of η can be decreased using Table 2.1. Otherwise, we have that η contains two columns composed by all bonds $(+,-)$. In this case, by looking at the last bond of the two columns in the internal boundary of Λ, we can prove that the energy of the configuration can be decreased taking advantage the zero-boundary conditions: see, indeed, the row five or the row nine of Table 2.1 and flip a minus to zero (row five) or a plus to zero (row nine). □

Before proving the remaining lemmas, we let the *local configuration* of the site x in η be the restricted configuration η_{U_x}, where $U_x = \{y \in \Lambda \,|\, |x-y| = 1\}$, see Fig. A.8 for some examples.

Proof of Lemma 4.5. Suppose that η does not contain bonds $(+,-)$, otherwise the statement follows from Lemma 4.4. Using Table 2.1, we find that the sole local configurations containing a plus whose energy cannot be decreased via a single flip are those depicted in Fig. A.8.

Let η be a configuration that contains at least a local configuration of type (V) in Fig. A.8. We consider η' obtained by flipping in η the minus to zero and the zero at the center to plus. Recalling that η does not contain bonds $(+,-)$, we have $H(\eta') < H(\eta)$ and $\Phi(\eta,\eta') - H(\eta) \le \lambda - h$.

Next, suppose that η is a configuration that contains at least a local configuration of type (VI). We consider η' obtained from η in three steps: we flip the two minuses to zero and then we flip the zero at the center to plus. Recalling that η does not contain bonds $(+,-)$, we have $H(\eta') \le H(\eta) + 2(\lambda - h) - (\lambda + h)$. By the assumption $h > \frac{\lambda}{2} > \frac{\lambda}{3}$, we have that $H(\eta') < H(\eta)$, and $\Phi(\eta,\eta') - H(\eta) \le 2(\lambda - h)$.

It follows that a cluster of pluses is composed solely by local configurations of types (I), (II), (III) with a plus at the center and only local configurations of type (IV) with a plus in the neighborhood, thus it is a rectangle. □

Proof of Lemma 4.6. Let η be a configuration as in the assumption. Suppose that the configuration does not contain bonds $(+,-)$, otherwise the statement follows from Lemma 4.4. We prove the result for the cluster of pluses, the other case is similar. Suppose that the cluster of pluses has at least one convex side with length $l_1 < \frac{2J}{\lambda+h}$. We flip the l_1 pluses along the side to zero decreasing in energy with a height smaller than or equal to $H(\eta)+(\lambda+h)(l_1-1) < H(\eta)+2J$, see row 13 in Table 2.1. Note that at each flip of the first $l_1 - 1$ steps, the energy increases by $\lambda + h$, since the number of the bonds between two equal spins does not change, although a plus is replaced by a zero. Finally, the effect of the last (l_1–th) flip is that of decreasing the energy by $2J - (\lambda + h)$, see row 12 in Table 2.1. □

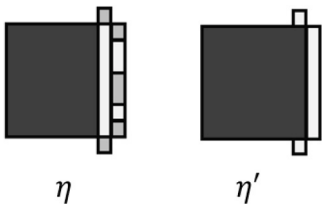

Fig. A.9. On the left, in black, an example of cluster of pluses of η with some minus spins at distance $\sqrt{2}$ and 2. On the right, the evolution of this cluster in η': all minuses at distance $\sqrt{2}$ and 2 from the cluster are replaced by zeros, and all zeros at distance one are replaced by pluses.

Proof of Lemma 4.7. Let η be a configuration as in the assumption. Suppose that η does not contain bonds $(+,-)$, otherwise the statement follows from Lemma 4.4. We prove the result for the cluster of pluses, the other case is similar. By assumptions, the rectangle of pluses has at least a side length $l_1 > \frac{2J}{\lambda+h}$ at distance strictly greater than two from a minus spin. We suppose that there are only zero spins at distance two from the pluses along this side, see Table 2.1. Then, we consider these l_1 zeros and we flip them to plus obtaining η' and decreasing in energy. In particular, the height of the path connecting η to η' is at most $2J - (\lambda + h) + H(\eta)$ (if the side is convex, otherwise $\Phi(\eta,\eta') = 0$ indeed if the side is concave then the energy decreases by $\lambda + h$ see Table 2.1 at row 13), see Table 2.1 at row 12. Indeed the first flip has an energy cost equal to $2J - (\lambda + h)$, since a zero is replaced by a plus and the number of the bonds between two equal spins has decreased by two. The other steps form a downhill path. Thus, denoted by $\underline{\omega}$ this path, we have $\Phi(\underline{\omega}) = 2J - (\lambda + h) + H(\eta) < 2J + H(\eta)$. □

Proof of Lemma 4.8. Let η be a configuration as in the assumption. Suppose that η does not contain bonds of type $(+,-)$ otherwise we conclude applying Lemma 4.4. Moreover, the cluster of pluses is a rectangle otherwise the statement is proven by Lemma 4.5. We consider a configuration η' obtained from η in the following way. All minuses at distance $\sqrt{2}$ and 2 from the side of the rectangle with length $l > \frac{2J+\lambda-h}{h}$ in η are replaced by zeros. Moreover, all zeros at distance one from the same side are replaced by pluses, see Fig. A.9. Next, we construct a path $\eta \to \eta'$ with $\Phi(\underline{\omega}) - H(\eta) < 5J$ and we show that $H(\eta') < H(\eta)$. In the worst case scenario, all spins at distance $\sqrt{2}$ and 2 from the rectangle are minuses. Thus, in particular we start flipping the two minuses at distance $\sqrt{2}$ from the side of the rectangle, and the energy increases by $2(\lambda - h)$. Next, we consider one of the l minuses at distance two from the considered side of the rectangle, and we flip it to zero. Then, we flip the nearest zero to plus. Starting from a minus at distance one from the minus considered before, we iterate these two steps ($-1 \to 0$ and $0 \to +1$) for $l - 1$ times obtaining η' such that $H(\eta') < H(\eta)$. Indeed, the first flip of the minus to zero has an energy cost of $2J + (\lambda - h)$ and the first flip of the zero to plus has an energy cost of $2J - (\lambda + h)$, see Table 2.1 at row 2 and 12 respectively. The rest of the steps has an energy cost of $\lambda - h$ when we flip a minus to zero and $-(\lambda + h)$ when we flip a zero to plus. Thus, we have $H(\eta') \le H(\eta) + 4J + 2(\lambda - h) - 2hl < H(\eta)$ since $l > \frac{2J+\lambda-h}{h}$, and the height along this path is $2(\lambda - h) + [2J + (\lambda - h)] + [2J - (\lambda + h)] + (\lambda - h) = 4J + 3\lambda - 5h < 5J$ since we chose $J \gg \lambda > h$. □

Proof of Lemma 4.9. We observe that if η contains a cluster of pluses with at least a side length $l > \frac{2J}{\lambda+h}$ at distance strictly greater than

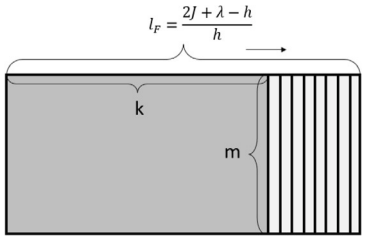

Fig. A.10. The rectangular cluster of pluses with side lengths k and m grows the side with length m for $l_F - k$ times. In this way we obtain a configuration containing a rectangular cluster of pluses with side lengths l_F and m.

two from a minus spin, then the proof is concluded by Lemma 4.7. Thus, suppose that there are some minuses at distance d smaller than or equal to two from the cluster of pluses. In particular $\sqrt{2} \le d \le 2$, otherwise there is a bond of type $(+,-)$ and we conclude the proof by Lemma 4.4. Moreover, the cluster of pluses is a rectangle, otherwise the proof is over by Lemma 4.5. We observe that the rectangle of pluses has both side lengths in $(\frac{2J}{\lambda+h}, \frac{2J+\lambda-h}{h})$, otherwise we conclude applying Lemma 4.6 or Lemma 4.8. Denote by $l_+ = \lceil \frac{2J}{\lambda+h} \rceil$ and $l_F = \lfloor \frac{2J+\lambda-h}{h} \rfloor$, moreover we indicate by $\tilde{l} = \lfloor \frac{J+\lambda+h}{h} \rfloor$. Next, we construct a path $\underline{\omega}$ from η to η', where η' is a configuration such that $H(\eta') < H(\eta)$ and $\Phi(\underline{\omega}) - H(\eta) < \Gamma$. In order to find η', we distinguish two cases. Let m, k be the two side lengths of the rectangle of pluses and we suppose $k \ge m$, then we have two possible cases:

(a) both sides have length strictly greater then $\tilde{l}$, that is $k, m \in [\tilde{l} + 1, l_F]$;
(b) at least one of two side lengths is smaller than $\tilde{l}$, that is $m \in [l_+, \tilde{l}]$.

In the first case, we obtain η' growing the rectangle of pluses as in proof of Lemma 4.8. In particular, we grow the side of the rectangle with length k for $l_F - k$ times, that is the rectangle grows up until it reaches the longer side length l_F. We observe that to grow the side of length k, we have to add m pluses along the side of length m, see Fig. A.10. We call $\tilde{\eta}$ this configuration. Along this first part $\eta \to \tilde{\eta}$ of the path $\eta \to \eta'$, the energy increases, because the rectangle is not supercritical. Then, we will grow up a supercritical rectangle until we obtain η' with $H(\eta') < H(\eta)$. Along this last part of path the energy decreases because it is a two-steps downhill path, so the height between η and η' is the same between η and $\tilde{\eta}$. Then, as proof of Lemma 4.8, we have $\Delta H(\text{side growth of length } m) \le 4J + 2(\lambda - h) - 2hm$. Thus, we obtain

$$\begin{aligned}
&\Delta H(\text{total growth}) \\
&\quad \le (l_F - k)\Delta H(\text{growth side of length } m) \\
&\quad \le \Big(\frac{2J+\lambda-h}{h} - k\Big)(4J + 2(\lambda - h) - 2hm). \qquad \text{(A.1)}
\end{aligned}$$

To find an upper bound to the communication height, we have to sum the energy difference from the rectangle with longer side length k to l_F with the energy cost to reach the rectangle with side length $l_F + 1$. In particular, we conclude finding the following upper bound

$$\begin{aligned}
&\Phi(\eta, \eta') - H(\eta) \\
&\le \sum_{j=k}^{l_F} \Delta H(\text{growth side of length } m) + (4J + 3\lambda - 5h) \\
&\le (4J + 2(\lambda - h) - 2hm)(l_F - k + 1) + (4J + 3\lambda - 5h) \\
&\le (4J + 2(\lambda - h) - 2h(\tilde{l} + 1))(l_F - \tilde{l}) + (4J + 3\lambda - 5h) \\
&< \Gamma.
\end{aligned}$$

where the second inequality follows from $k, m \ge \tilde{l}$, and the last one follows from $\tilde{l} = \lfloor \frac{J+\lambda+h}{h} \rfloor$ and $J \gg \lambda > h$.

In the second case, we obtain η' shrinking the rectangle of pluses as in proof of Lemma 4.6. In particular, we cut the side of the rectangle with length m until the cluster of pluses is replaced by a cluster of zeros, see Fig. A.11. First of all, we prove that $H(\eta') < H(\eta)$. We observe that $k \le l_F < \frac{2Jm}{(\lambda+h)m-2J}$, where the second inequality is due to $h > \frac{\lambda}{2}$, and then we have $H(\eta) - H(\eta') = 2J(k+m) - (\lambda+h)km > 0$.

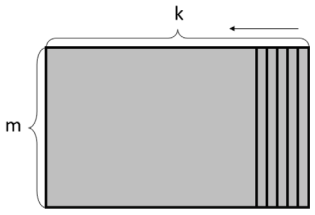

Fig. A.11. The rectangular cluster of pluses with side lengths k and m shrinks until it is totally replaced by a rectangular cluster of zeros with the same size.

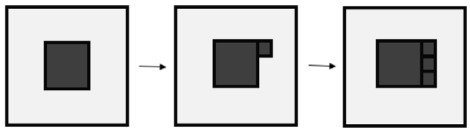

Fig. A.12. A part of the path $\underline{\omega} : \mathbf{0} \mapsto \mathbf{+1}$. The white part represents the region with zero spins, the black region is the cluster of pluses. We remark that the first flip from zero to plus can occur at any site of Λ with the same probability, this is the case of the homogeneous nucleation.

To find an upper bound for the communication height, first of all we compute the energy to cut a side of the rectangle and the height along this part of the path $\underline{\omega}$. For the first $k - 1$ times, we have $\Delta H(\text{shrink side of length } m) = (\lambda+h)m - 2J$. And $\Phi(\underline{\omega}) - H(\eta) = (\lambda+h)m$. Indeed, when we cut $k-1$ sides of length m, we obtain a configuration with a rectangle $1 \times m$, so the path toward η' is a downhill path. Thus,

$$\begin{aligned}
&\Phi(\eta, \eta') - H(\eta) \\
&\quad \le \sum_{j=1}^{k-2} \Delta H(\text{shrink side of length } m) + (\lambda + h)m \\
&\quad = [(\lambda + h)m - 2J](k - 2) + (\lambda + h)m \\
&\quad < [(\lambda + h)\tilde{l} - 2J](l_F - 2) + (\lambda + h)\tilde{l} < \Gamma,
\end{aligned}$$

where for the first inequality we used $m \le \tilde{l}$ and $k \le l_F$. The second inequality follows from the values of $\tilde{l}$, l_F and the assumption $h > \frac{\lambda}{2}$, $J \gg \lambda > h$. □

Proof of Lemma 4.10. To prove the result, we provide a path from **0** to **+1**. We define our path $\underline{\omega} : \mathbf{0} \mapsto \mathbf{+1}$ as a sequence of configurations from **0** to **+1** with increasing clusters *as close as possible to quasi-square*, see Fig. A.12. We construct a path in which at each step we flip one spin from zero to plus. We flip the spin at the origin and then we add clockwise three square units to obtain the first square with side length $l = 2$. Then we flip the zero spins on the top of the square 2×2, adding consecutive square units until we obtain a quasi-square 2×3. Next we flip the zero spins along the longest side to obtain a square 3×3. We go on in the same manner flipping consecutive zero spins at distance one to the cluster of pluses. We iterate this nucleation process until the quasi-square takes up all the space Λ. In the following we compute the height of this procedure. First of all, we compute the energy cost between the configuration **0** and a configuration with a rectangular cluster of pluses with side lengths m and n, called $\sigma_{m,n}$,

$$H(\sigma_{m,n}) - H(\mathbf{0}) = 2J(n+m) - (\lambda+h)mn \qquad \text{(A.2)}$$

where $2(m+n)$ is the number of bonds $(0,+)$ and mn is the number of pluses in $\sigma_{m,n}$. Eq. (A.2) attains the maximum for $(m,n) = \Big(\frac{2J}{\lambda+h}, \frac{2J}{\lambda+h}\Big)$, that corresponds to a configuration with a quasi-square of pluses with side lengths $\tilde{n} = \lfloor \frac{2J}{\lambda+h} \rfloor$ and $\tilde{n} + 1$. Starting from $\sigma_{\tilde{n},\tilde{n}+1}$ to reach the

configuration $\sigma_{\tilde{n}+1,\tilde{n}+1}$, the energy cost is given by the first step and its value is $2J-(\lambda+h)$, see Table 2.1 at row 12, the rest of the path is a downhill path. Thus, recalling that $H(\mathbf{0})=0$, using the value of $\tilde{n}$ and the assumption $\lambda>h$, we have

$$\begin{aligned}&\Phi(\mathbf{0},\mathbf{+1})-H(\mathbf{0})\\&\leq \Phi(\sigma_{\tilde{n},\tilde{n}+1},\sigma_{\tilde{n}+1,\tilde{n}+1})-H(\mathbf{0})\\&=H(\sigma_{\tilde{n},\tilde{n}+1})+2J-(\lambda+h)-H(\mathbf{0})\\&<\frac{4J^2}{\lambda+h}+2J+(\lambda+h)<\frac{2J^2}{h}+\frac{2J\lambda}{h}-3h<\Gamma.\end{aligned}$$ □

A.2. Proofs of lemmas of Section 4.5.2

We first state few preliminary results necessary to prove Lemmas. 4.11–4.13, and then we report the proofs of these lemmas. We start by simple result which is an immediate corollary of Lemma 4.7.

Corollary A.1. *Let η be a configuration that contains a strip of minuses with at least a side length $l>\frac{2J}{\lambda-h}$ at distance strictly greater than two from a plus spin. Then $V_\eta<2J$.*

Lemma A.19. *Let $\eta\in\mathcal{M}_{n_c^+}$ be a configuration that contains a rectangle R with side lengths $l_1,l_2>\lfloor\frac{2J}{\lambda-h}\rfloor+2$ with inside no plus spins. Assume that $\eta_{R\setminus\partial^- R}\neq\mathbf{-1}_{R\setminus\partial^- R}$. If $\eta(x)=-1$ for at least a site $x\in R\setminus\partial^- R$, then there exists a configuration $\eta'\in\mathcal{M}_{n_c^+}$ such that $H(\eta')<H(\eta)$.*

Lemma A.20. *Let $\eta\in\mathcal{M}_{n_c^+}$ be a configuration that contains a rectangle R with side lengths $l_1,l_2>\lfloor\frac{4J}{\lambda-h}\rfloor+2$ with inside no plus spins. Let $S=R\setminus\partial^- R$ and $\eta(x)=0$ for every $x\in S$, then the configuration $\eta'\in\mathcal{M}_{n_c^+}$ such that $\eta'_{\Lambda\setminus S}=\eta_{\Lambda\setminus S}$ and $\eta'_S=\mathbf{-1}_S$ has $H(\eta')<H(\eta)$.*

Proof of Corollary A.1. If a configuration contains a strip of minuses as in the assumptions, then there exists a cluster of minuses containing this strip with at least a side length $l>\frac{2J}{\lambda-h}$ at distance strictly greater than two from a plus spin, then we conclude by applying Lemma 4.7. □

Proof of Lemma A.19. Let η be a configuration as in the assumptions. We distinguish two cases: (i) η contains at least a cluster of minuses with shape different from a rectangle, (ii) η contains only cluster of minuses with rectangular shape. In the first case, there is at least a zero spin with two minus spins at distance one, then we find η' by using Table 2.1 at row 4 (by flipping this zero in to a minus). In the second case, we find η' by applying either Lemma 4.6 or Lemma 4.7, according to the side length of the cluster of minuses. □

Proof of Lemma A.20. Consider η and η' as in the assumption. The energy difference between η and η' is given by

$$\begin{aligned}&H(\eta')-H(\eta)\\&=2J(l_1-2+l_2-2)-(\lambda-h)(l_1-2)(l_2-2)\\&<2J\frac{8J}{\lambda-h}-(\lambda-h)\Big(\frac{4J}{\lambda-h}\Big)^2=0.\end{aligned}$$

To compute the height $\Phi(\eta,\eta')$, we argue as in proof of Lemma 4.10. Indeed the computation of $\Phi(\eta,\eta')$ is similar to one of $\Phi(\mathbf{0},\mathbf{+1})$, hence it is strictly smaller than Γ. □

Proof of Lemma 4.11. Let η be a configuration as in the assumption and we suppose by contradiction that $\eta\in M$. First of all, we observe that if η contains at least one of the local configurations in Fig. A.13 (or one of their rotations), then there exist $\eta'\in\mathcal{M}_{n_c^+}$ such that $H(\eta')<H(\eta)$ by using Table 2.1, thus $\eta\notin M$.

From now on, we suppose that η does not contain the previous local configurations in Fig. A.13. For the assumption, η contains at least a column (or a row) with only zero spins, then η contains at least one of the configurations in Fig. A.14.

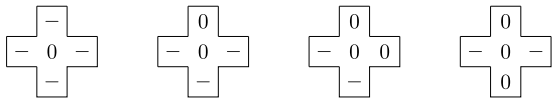

Fig. A.13. If η contains one of these local configuration, then it reducible in energy by flipping the zero in the center in to minus, see Table 2.1.

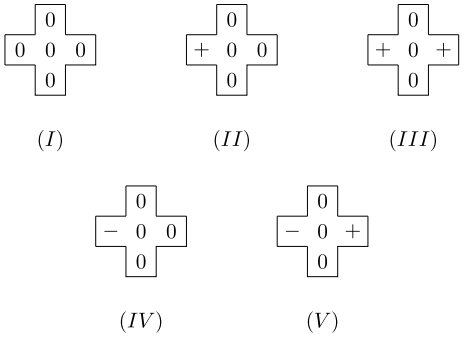

Fig. A.14. Local configurations with the center site along a column filled by only zero spins.

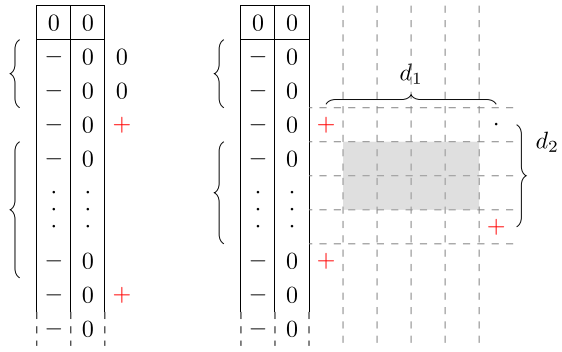

Fig. A.15. Neighborhood of the column with only zeros spins with attached a strips of minuses.

We observe that η does not contain only local configurations of type (I) among those in Fig. A.14, indeed $\eta\in\mathcal{M}_{n_c^+}$. Moreover, we show that if η contains only local configurations of type (I) and (II) among those in Fig. A.14, then $\eta\notin M$. Indeed, in this case η does not contain minus spins and by [42] we have $H(\eta)\geq H(\xi)$ where ξ is the configuration with a quasi-square of pluses in a sea of zeros, and for L large enough we have $H(\xi)=4J(2l_c-1)-(\lambda+h)l_c(l_c-1)$ and $H(\sigma_c)=4J(2l_c-1)-(\lambda+h)l_c(l_c-1)+4JL-(\lambda-h)(L^2-l_c(l_c-1)-(2l_c-1))$, implying $H(\xi)>H(\sigma_c)$ and $\eta\notin M$. With the same argument, we may state that if η contains only local configurations of type (I), (II) and (III) among those in Fig. A.14, then $\eta\notin M$.

Thus, we suppose that η contains at least a local configurations of type (IV) or (V) and we start to analyze the two columns (or rows) that contain the pair $(-,0)$ until we find a pair $(\eta(x),0)$ such that $\eta(x)\neq-1$. First of all, we observe that if the strip of minuses in the first column has a length smaller than $\frac{2J}{\lambda-h}$, then there exists a configuration $\eta'\in\mathcal{M}_{n_c^+}$ with $H(\eta')<H(\eta)$ by Lemma 4.6, and so $\eta\notin M$. Moreover, if $\eta(x)=+1$ then we find $\eta'\in\mathcal{M}_{n_c^+}$ such that $H(\eta')<H(\eta)$ by using Table 2.1, and also in this case $\eta\notin M$. Thus, the unique possible pair $(\eta(x),0)$ is $(0,0)$. In this case, there is a plus spin at distance two from the strip of minuses, otherwise η satisfies the assumptions of Corollary A.1 and so $\eta\notin M$, see Fig. A.15.

Moreover, for every configuration that contains a pair of two consecutive columns filled by minuses and zeros, there are some plus spins

that split the strips of minuses in parts with length smaller than $\frac{2J}{\lambda-h}$, see Fig. A.15 for an example, otherwise we can reduce the energy of η by applying Corollary A.1, and so $\eta \notin M$. This implies that the distance between two pluses at distance two from the strip of minuses is smaller than $\frac{2J}{\lambda-h}$, see Fig. A.15.

Starting from the pair $(0,0)$, we focus on the first plus at distance two from the column of minuses and we consider the plus in the nearest column, see Fig. A.15. We observe that the region between these pluses contains only zero and minus spins for construction. In the following, we will prove that this region is a rectangle with both side lengths smaller than $\lfloor\frac{4J}{\lambda-h}\rfloor+2$. Indeed, if this region is a rectangle with side length greater than $\lfloor\frac{4J}{\lambda-h}\rfloor+2$ and it contains only zero spins, then we can apply Lemma A.20 and so $\eta \notin M$. However, if this region contains some minus spin then we may apply Lemma A.19, indeed the assumption and $\eta_{R\setminus\partial^+R} \neq -\mathbf{1}_{R\setminus\partial^+R}$ is satisfied otherwise η contains the last local configuration in Fig. A.13. Hence, the considered region is a rectangle with both side lengths smaller than $\lfloor\frac{4J}{\lambda-h}\rfloor+2$. Let d_1 be the distance between the two columns containing the two plus spins, d_2 be the distance between the two rows containing the two plus spins, then $d_1, d_2 < \lfloor\frac{4J}{\lambda-h}\rfloor+2$, see Fig. A.15. Thus, the Euclidean distance between the two pluses has to be smaller than $\sqrt{2}\left(\lfloor\frac{4J}{\lambda-h}\rfloor+2\right)$. So, we can compute the maximal size of the minimal rectangle containing all plus spins. Indeed the diagonal of this rectangle is $n_c^+\sqrt{2}\left(\lfloor\frac{4J}{\lambda-h}\rfloor+2\right)$ and its side lengths are smaller than $l_R = n_c^+\left(\lfloor\frac{4J}{\lambda-h}\rfloor+2\right)$.

Let $\tilde\partial^+R = \partial^+R \cup \{x \in \Lambda\setminus R \,:\, |x-y| = \sqrt{2} \;\; \forall\, y \in R\}$, the region $\Lambda\setminus(R\cup\tilde\partial^+R)$ can be composed by two, three or four rectangles that circumscribing R, see Fig. A.16. We consider the rectangle R_M with maximal area among them and we prove that it has side lengths strictly greater than $\lfloor\frac{4J}{\lambda-h}\rfloor+2$. The maximal rectangle contained in $\Lambda\setminus(R\cup\tilde\partial^+R)$ has side lengths (L,x) with $x \geq \frac{L}{2} - n_c^+\left(\lfloor\frac{4J}{\lambda-h}\rfloor+2\right)-1$. In particular, we have $L,x > \lfloor\frac{4J}{\lambda-h}\rfloor+2$, since $L > \left(\frac{2J}{\lambda-h}\right)^3$. Therefore, for every position of R in Λ, there is a rectangle R_M that contains only minus spins, otherwise it satisfies the assumption of either Lemma A.19 or Lemma A.20, and so $\eta \notin M$. Moreover, there is a strip of minus with length $y > \lfloor\frac{2J}{\lambda-h}\rfloor$, see Fig. A.16, attached to R_M. Thus, the rectangle S_M attached to R_M, see Fig. A.16, is filled by only minus spins, otherwise we can apply Corollary A.1 and $\eta \notin M$. Follows that the column with length L filled by only zero spins is not in $\Lambda\setminus(R\cup\tilde\partial^+R)$, then it is in $\tilde\partial^+R\cup R$. However, every column (and row) in $\tilde\partial^+R\cup R$ has length strictly smaller than L, thus it is a contradiction. We can conclude $\eta \notin M$. □

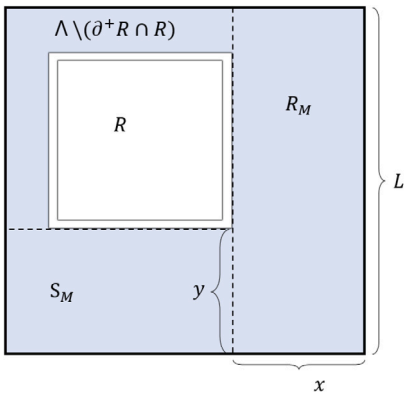

Fig. A.16. The minimal value of x and y is $\frac{L}{2} - n_c^+\left(\lfloor\frac{4J}{\lambda-h}\rfloor+2\right)-1$, when R centered in the middle of Λ. In each case $L,x > \lfloor\frac{4J}{\lambda-h}\rfloor+2$.

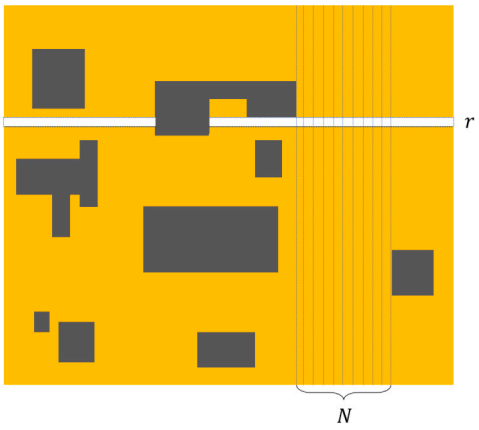

Fig. A.17. The cluster of pluses are in dark gray. The white region indicates the zero region, while the yellow region contains a mixture of zeros and minuses. The set of the N column without pluses that intersect r is the rectangle $R_{L,N}$.

Proof of Lemma 4.12. Let η be a configuration as in the assumption and suppose by contradiction that $\eta \in M$. Let n_η^0 be the number of the zero spins in η. We first show that if a column or a row contains only plus and zero spins, then $\eta \notin M$. Suppose that η contains a row r with only plus and zero spins and we consider the maximal sequence of $N > 0$ consecutive columns that intersects r without plus spins. This set of consecutive columns forms a rectangle $R_{L,N}$ and we note that $N > \lfloor\frac{2J}{\lambda-h}\rfloor+2$, indeed $\frac{L}{n_c^+} > \lfloor\frac{2J}{\lambda-h}\rfloor+2$ see Condition 1. If one of them contains only zero spins, then $\eta \notin M$ by Lemma 4.11. Thus, we may apply Lemma A.19 and we obtain $\eta \notin M$.

Follows that, for each column and row that contains at least plus, one of the following conditions holds:

(a) there are two bonds $(+,0)$ and at least two bonds $(-,0)$. No bond $(+,-)$ is present. In this case the energy contribution is at least $4J$, by the definition of the Hamiltonian function (2.1), and we denote by α_1 the number of these columns and rows. See Fig. A.17.

(b) there are a bond $(+,-)$, at least a bond $(-,0)$ and a bond $(+,x)$ where $x \in \{-1,0\}$. No more than one bond $(+,0)$ is present. The energy contribution is at least $6J$ and we denote by α_2 the number of these columns and rows. See Fig. A.17.

(c) there are either at least four bonds $(+,0)$ and at least two bonds $(-,0)$, or at least a bond $(+,-)$, at least a bond $(-,0)$ and more than one bond $(+,x)$ where $x \in \{-1,0\}$. The energy contribution is at least $6J$ and we denote by α_3 the number of these columns and rows. See Fig. A.17

Moreover, we observe that in η there are no column filled with only zero spins, otherwise we apply Corollary A.1. Then, the energy contribution along every column and every row is at least $2J$ according to the zero-boundary conditions. We denote by α_4 the number of these columns and rows.

We note that $\sum_{i=1}^4 \alpha_i = 2L$, since we found a partition of the set of columns and rows in Λ according to the presence or the absence of pluses. Moreover, we observe that by [42] a cluster of pluses with fixed area $n_c^+ = l_c(l_c-1)$ has perimeter $p \geq 2(2l_c-1)$. In particular, the cluster with area n_c^+ has minimal perimeter if and only if it is a quasi-square with semi-perimeter $2l_c-1$. In our case, the cluster of pluses has area n_c^+ and a shape different from a quasi-square for assumption, then its semi-perimeter is strictly greater than $2l_c-1$. We note that the semi-perimeter of such cluster coincide with the number of columns and rows with a plus, that is $\sum_{i=1}^3 \alpha_i \geq 2l_c-1$.

Let n_η^- be the number of minuses in η, we can write the energy function of η as

$$H(\eta) \geq 4J\alpha_1 + 6J\alpha_2 + 6J\alpha_3 + 2J\alpha_4 - n_c^+(\lambda+h) - n_\eta^-(\lambda-h), \tag{A.3}$$

and we have

$$H(\eta) \geq 4J(\alpha_1+\alpha_2+\alpha_3) + 2J(\alpha_2+\alpha_3)$$

$$
\begin{aligned}
&+2J(2L-\alpha_1-\alpha_2-\alpha_3)-n_c^+(\lambda+h)-n_\eta^-(\lambda-h)\\
&=2J(\alpha_1+\alpha_2+\alpha_3)+2J(\alpha_2+\alpha_3+2L)\\
&-n_c^+(\lambda+h)-n_\eta^-(\lambda-h).
\end{aligned}
\tag{A.4}
$$

Recalling the remark below (4.25), we rewrite the energy of σ_c and in the following we compare $H(\sigma_c)$ with the energy of η in (A.4).

$$
\begin{aligned}
H(\sigma_c)&=4J(2l_c-1)+2J(2L-(2l_c-1))\\
&\quad-n_c^+(\lambda+h)-n_\sigma^-(\lambda-h)\\
&=2J(2l_c-1)+4JL-n_c^+(\lambda+h)-n_{\sigma_c}^-(\lambda-h).
\end{aligned}
\tag{A.5}
$$

We distinguish two cases according to the number of zeros in η: $k > 2l_c-1=n_{\sigma_c}^0$ and $k\le 2l_c-1=n_{\sigma_c}^0$. In the first case, by (A.4) and recalling $\sum_{i=1}^3\alpha_i\ge 2l_c-1$, we obtain

$$
\begin{aligned}
&H(\eta)-H(\sigma_c)\\
&\ge 2J(\alpha_2+\alpha_3)+(n_{\sigma_c}^- - n_\eta^-)(\lambda-h)\\
&=2J(\alpha_2+\alpha_3)+(n_\eta^0-n_{\sigma_c}^0)(\lambda-h)>0
\end{aligned}
\tag{A.6}
$$

since $\alpha_2,\alpha_3\ge 0$ and $n_\eta^0-n_{\sigma_c}^0>0$.

In the second case, we observe that η has to contain a bond $(+,-)$ since the semi-perimeter of its cluster of pluses is strictly greater than $2l_c-1$ and the number of zeros k is smaller than $2l_c-1$. This means that either $\alpha_2\ge 1$ or $\alpha_3\ge 1$. In particular, if $\alpha_3=0$ (and $\alpha_1\ge 1$) then η contains a single cluster of pluses with a shape different from a quasi-square and in this case $\alpha_1+\alpha_2>2l_c-1$. Hence, by using (A.4) and (A.5), we obtain

$$
\begin{aligned}
H(\eta)-H(\sigma_c)&>2J(\alpha_2+\alpha_3)+(n_{\sigma_c}^- - n_\eta^-)(\lambda-h)\\
&\ge 2J+(n_\eta^0-n_{\sigma_c}^0)(\lambda-h)\\
&=2J+(k-2l_c+1)(\lambda-h)\\
&\ge 2J+(2-2l_c)(\lambda-h)\ge 0
\end{aligned}
\tag{A.7}
$$

where the last inequality follows by (3.16), $k\ge 1$ and $J\gg\lambda>h>\frac{\lambda}{2}$.

Otherwise, if $\alpha_3\ge 1$ we note that η contains at least two disconnected clusters of pluses and for the geometry of the lattice, also in this case we have $\alpha_1+\alpha_2>2l_c-1$. Thus, arguing as above, we obtain the same result as in (A.7). □

Proof of Lemma 4.13. Let $\eta\in\operatorname{argmax}_{\xi\in\mathcal{M}_{n_c^+}}H(\xi)$. By Lemma 4.12 we have that η contains a single quasi-square Q of pluses. Moreover, we may apply Lemma A.19 or Lemma A.20 in the region $\Lambda\setminus Q$, then we have $\eta_{\Lambda\setminus(Q\cup\partial^+Q)}=-1_{\Lambda\setminus(Q\cup\partial^+Q)}$, otherwise $\eta\notin M$. □

Proof of Lemma 4.14. Let $\eta\in\mathcal{M}_{n_c^+}$. By Lemma 4.13, we have that $\eta_Q=+1_Q$ and $\eta_{\Lambda\setminus(Q\cap\partial^+Q)}=-1_{\Lambda\setminus(Q\cap\partial^+Q)}$, otherwise $\eta\notin M$. We will prove that if $\eta\in M$, then $\eta_{\partial^+Q}=0_{\partial^+Q}$. Suppose that there exists $x,y\in\partial^+Q\cap\Lambda$, $|x-y|=1$, such that $\eta(x)=0$ and $\eta(y)=-1$, then we find $\eta'\in\mathcal{M}_{n_c^+}$ with $H(\eta')<H(\eta)$ by applying Table 2.1 at row 5 (by flipping the minus in y in to zero). Then, we have either $\eta(x)=-1$ for all $x\in\partial^+Q\cap\Lambda$, or $\eta(x)=0$ for all $x\in\partial^+Q\cap\Lambda$. However, in the first case there exists $x,y\in\partial^+Q\cap\Lambda$, $|x-y|=1$, such that $\eta(x)=\eta(y)=-1$, then by flipping the two minuses in x and y into zero, we obtain a configuration $\eta'\in\mathcal{M}_{n_c^+}$ with $H(\eta')=H(\eta)-2J+2(\lambda-h)<H(\eta)$ by applying Table 2.1 at rows 3 and 5. Thus, $\eta_{\partial^+Q\cap\Lambda}=0_{\partial^+Q\cap\Lambda}$ otherwise $\eta\notin M$.

According to the zero-boundary conditions, the energy of η depends on the position of Q, then η can contain either a frame, or a chopped boundary frame or a chopped corner frame. The energy of these three configuration is computed in (3.13) and by using (3.14), we can conclude that σ_c is the unique $\operatorname{argmax}_{\xi\in\mathcal{M}_{n_c^+}}H(\xi)$. □

Lemma A.21. *If $\underline{\omega}$ is a path from σ_c to $\mathcal{M}_{n_c^++1}$ such that $\underline{\omega}=(\sigma_c,\eta_1,\eta_2,\dots,\eta_n)$, $n\ge 1$, with $\eta_n\in\mathcal{M}_{n_c^++1}$ and $\eta_i\in\mathcal{M}_{n_c^+}$ for every $i=1,\dots,n-1$, then $\Phi(\underline{\omega})\ge H(\tilde\sigma_c)$.*

Proof of Lemma A.21. Consider a path $\underline{\omega}$ as in the assumption, and we suppose by contradiction that $\Phi(\underline{\omega})<H(\tilde\sigma_c)$. If there exists $\eta\in\mathcal{M}_{n_c^++1}\cap\underline{\omega}$ such that $\sigma_c\sim\eta$, then by Table 2.1, we obtain

$$
\Phi(\underline{\omega})\ge H(\eta)=H(\sigma_c)+4J-(\lambda+h)>H(\tilde\sigma_c).
\tag{A.8}
$$

Then, we have $\sigma_c\sim\eta$ where $\eta\in\mathcal{M}_{n_c^+}\cap\underline{\omega}$. We note that, according to Table 2.1, if the configuration contains a cluster of pluses with a quasi-square shape, then the minimal energy contribution to add a plus is $2J-(\lambda+h)$. This is possible by flipping a zero with $\begin{smallmatrix}&0&\\0&\cdot&0\\&0&\end{smallmatrix}$ nearest neighbors into a plus, however all zero spins in σ_c have only a plus and at most two zeros nearest neighbors. Thus, we obtain η from σ_c by flipping a minus into zero in order to create a zero with $\begin{smallmatrix}&0&\\0&\cdot&0\\&0&\end{smallmatrix}$ nearest neighbors, otherwise $\Phi(\underline{\omega})\ge H(\tilde\sigma_c)$. We note that the minimal energy contribution to obtain η is $(\lambda-h)$ when we flip a minus with at most two minuses nearest neighbors to zero, see Table 2.1. Then, we obtain from η a configuration $\eta'\in\mathcal{M}_{n_c^+}$ by adding a plus in the site where there is the zero with $\begin{smallmatrix}&0&\\0&\cdot&0\\&0&\end{smallmatrix}$ nearest neighbors. However, also in this case we have $\Phi(\underline{\omega})\ge H(\eta')=H(\sigma_c)+(\lambda-h)+2J-(\lambda+h)=H(\tilde\sigma_c)$ and this is a contradiction. We observe that if we remove more than one minus before adding a plus, the height is even greater. □

Proof of Lemma 4.15. Let $\underline{\omega}=(\eta_1,\dots\eta_n)$, $n\in\mathbb{N}$, be a path as in the assumption. We consider the part of $\underline{\omega}$ from $\mathcal{M}_{n_c^+}$ to $\mathcal{M}_{n_c^++1}$ and let $\eta_i\in\mathcal{M}_{n_c^+}\cap\underline{\omega}$ such that $\eta_i\sim\eta_{i+1}\in\mathcal{M}_{n_c^++1}$. By the assumption $\eta_i\not\equiv\sigma_c$, and we assume by contradiction that $\Phi(\underline{\omega})\le H(\tilde\sigma_c)$. By applying Lemma 4.14 we have $H(\eta_i)>H(\sigma_c)$, and in particular from Table 2.1 since $\eta_i\not\equiv\sigma_c$ we have $H(\eta_i)=H(\sigma_c)+2Ja+b(\lambda-h)$ with $a\in\mathbb{N}$ and $b\in\mathbb{Z}$ such that $2Ja+b(\lambda-h)>0$. Moreover, $H(\eta_i)\le\Phi(\underline{\omega})\le H(\tilde\sigma_c)$. Then, by (4.26) we have $H(\eta_i)\le\Phi(\underline{\omega})\le H(\tilde\sigma_c)=H(\sigma_c)+2J+(\lambda-h)$, where we used (4.26). It follows that $a<0$ and $b<0$ and this is a contradiction since we assumed $2Ja+b(\lambda-h)>0$. □

Proof of Lemma 4.16. Let $\underline{\omega}$ be a path from $\tilde\sigma_c\in\mathcal{M}_{n_c^++1}$ to $\mathcal{M}_{n_c^++2}$ without loops. Then, if there exists $\eta\sim\tilde\sigma_c$ such that $\eta\in\underline{\omega}\cap\mathcal{M}_{n_c^++2}$ then by Table 2.1, we have $\Phi(\underline{\omega})\ge H(\tilde\sigma_c)+2J-(\lambda+h)$ and we conclude by (4.26) and (4.27). Otherwise, if along $\underline{\omega}$ we have that $\tilde\sigma_c\sim\eta$ with $\eta\in\mathcal{M}_{n_c^++1}$ then we conclude $\Phi(\underline{\omega})\ge H(\tilde\sigma_c)+(\lambda-h)$ by using Table 2.1, (4.26) and (4.27). □

Proof of Lemma 4.17. Let $\eta\in\mathcal{M}_{n_c^++1}$ be a configuration such that $H(\eta)=H(\tilde\sigma_c)$. Then, by using the same partition of the columns and rows in the proof of Lemma 4.12 (see conditions a, b, c and Fig. A.17, we have

$$
\begin{aligned}
&H(\eta)-H(\tilde\sigma_c)\\
&\quad=4J(\alpha_1-2l_c)+2J(\alpha_4-2L+2l_c)\\
&\qquad+6J(\alpha_2+\alpha_3)+(n_c^- - n_\eta^-)(\lambda-h)\\
&\quad=2J(2\alpha_1+\alpha_4+3\alpha_2+3\alpha_3-2L-2l_c)\\
&\qquad+(n_c^- - n_\eta^-)(\lambda-h).
\end{aligned}
$$

Since $H(\eta)=H(\tilde\sigma_c)$, it follows that $2\alpha_1+\alpha_4+3(\alpha_2+\alpha_3)=2(L+l_c)$ and $n_c^-=n_\eta^-$. The second equality implies that the number of minuses in η is the same as in $\tilde\sigma_c$. Recalling that $\sum_{i=1}^4\alpha_i=2L$, we obtain $\alpha_1+2(\alpha_2+\alpha_3)=2l_c$. Moreover, $\sum_{i=1}^3\alpha_i\ge 2l_c$ indeed the minimal semi-perimeter of a cluster of pluses with area n_c^+ is $2l_c$ by [42]. Then, we derives $\alpha_2+\alpha_3=0$. From the definitions of α_2 and α_3, it follows that the bonds of type $(+,-)$ are not present and that the number of bonds $(+,0)$ in each column and row is at most two. Hence, $\alpha_1=2l_c$ and $\alpha_4=2(L-l_c)$. This implies that the union of the clusters of pluses has a semi-perimeter equal to $2l_c$. By [42], such union of clusters has to be

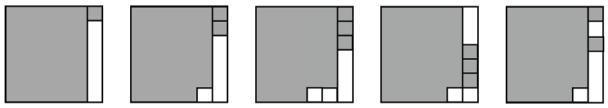

Fig. A.18. Examples of clusters of pluses with area n_c^+ and the same perimeter of a square with side length l_c. The first three clusters are contained in a configuration of $\mathcal{S}$.

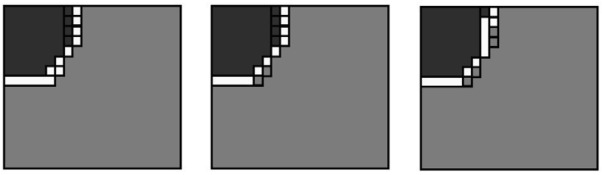

Fig. A.19. On the left, a configuration $\eta \in \mathcal{S}$. In the middle η_k, with $k = 2$ in this case. On the right, an example of the configuration η_m with $m = 3$ and such that $H(\eta_m) = H(\eta_k) + m(\lambda + h) - (m-1)(\lambda - h)$.

contained either in a square with both side length l_c or in a rectangle with side length $l_c - 1$ and $l_c + 1$. Moreover, the cluster of pluses cannot contain more than one protuberance along each side (otherwise $\alpha_3 \neq 0$), see Fig. A.18. We note that the cluster is in the corner of Λ, otherwise either the number of zeros is greater than the number of zeros in $\tilde{\sigma}_c$, or η contains at least a bond $(+,-)$. Finally, we observe that in case the configuration contains more than one strip of minuses in at least a column or a row of Λ, then η contains a column among the α_4 columns with an energy contribution of $4J$ instead of $2J$ and so $H(\eta) > H(\tilde{\sigma}_c)$. For the same reason, the protuberance attached to the cluster is at distance one from the boundary of Λ, see Fig. A.18. We may conclude that $\eta \in \mathcal{S}$. □

Proof of Lemma 4.18. We consider a configuration $\eta \in \mathcal{S} \setminus \{\tilde{\sigma}_c\}$. By the property of $\mathcal{S}$, the cluster of pluses of every configuration in $\mathcal{S}$ has perimeter equal to $2l_c$, but the number of the sites along the external-boundary of this cluster (the so called *site-perimeter*) changes according to the number of its concave angles. We note that $\tilde{\sigma}_c$ contains $2l_c$ sites along the external-boundary of the cluster of pluses, instead the other configurations contains $k > 1$ concave angles (see the second and the third pictures in Fig. A.18 for two examples with $k = 2$). Moreover, every configuration in $\mathcal{S}$ contains $2l_c$ zero spins, thus $\eta \neq \tilde{\sigma}_c$ contains $k \geq 1$ zero spins at distance strictly greater than one from the cluster. In particular, this zero spins are in the minimal rectangle containing the cluster of pluses and they are attached from the zero spins at distance one from the cluster in order not to create more than one strip of minuses in each column and row of Λ.

We consider the configuration η_k obtained from η by flipping these k zero spins to minus, see Fig. A.19. For the definition of the set $\mathcal{S}$ and by using Table 2.1, we have $H(\eta_k) = H(\eta) - k(\lambda - h)$. By Table 2.1, we note that η_k is a local minimum, indeed every path from it is an up-hill path. In particular, since to reach $-\mathbf{1}$, $\underline{\omega}$ must cross all the manifold $\mathcal{M}_{n_c^+ + 1}$, $\mathcal{M}_{n_c^+}$, $\mathcal{M}_{n_c^+ - 1}$, …, $\mathcal{M}_0$, then we consider η_m be the configuration with a protuberance with cardinality one obtained from η_k, see Fig. A.19 for an example of η_m. The path that connected η_k with η_m is a two-steps down-hill path, where the up-hill is the minimal positive energy quantum $\lambda - h$, thus $\Phi(\eta, \eta_m) \geq \Phi(\underline{\omega})$. We obtain $H(\eta_m) = H(\eta_k) + m(\lambda + h) - (m-1)(\lambda - h)$ by flipping m pluses to zero and $m - 1$ zeros to minus as in Fig. A.19 and by using Table 2.1. We note that $m \geq k$, indeed the cluster of pluses contains $n_c^+ + 1$ pluses in a rectangle $l_c \times l_c$ (or $(l_c - 1) \times (l_c + 1)$) then when it contains γ concave angles then the protuberance has cardinality more than γ because the pluses that are not present in the sites of the concave angles must be located along the protuberance to be inside the rectangle.

Assume by contradiction that $\Phi(\underline{\omega}) \leq H(\sigma_s)$. Thus, we have

$$\begin{aligned} H(\sigma_s) &\geq H(\eta_m) \geq H(\eta_k) + m(\lambda + h) - (m-1)(\lambda - h) \\ &\geq H(\eta) - (k + m - 1)(\lambda - h) + m(\lambda + h) \\ &= H(\tilde{\sigma}_c) - (k + m - 1)(\lambda - h) + m(\lambda + h) \\ &\geq H(\tilde{\sigma}_c) + (1 - k)\lambda + (2m + k - 1)h \\ &= H(\sigma_s) - k\lambda + (2m + k)h \\ &\geq H(\sigma_s) - k\lambda + 3kh \end{aligned} \tag{A.9}$$

where the equality is obtained by (4.26) and (4.27) and the last inequality follows from $m \geq k$. Then, we obtain a contradiction, indeed $H(\sigma_s) \geq H(\sigma_s) - k\lambda + 3kh \geq H(\sigma_s) - \lambda + 3h > H(\sigma_s)$, since $k \geq 1$ and $h > \lambda/2$. □

References

[1] M. Blume, Theory of the first–order magnetic phase change in UO_2, Phys. Rev. 141 (1966) 517.
[2] H.W. Capel, On possibility of first–order phase transitions in ising systems of triplet ions with zero-field splitting, Physica 32 (1966) 966.
[3] S.-A. Muntean, V. Kronberg, M. Colangeli, A. Muntean, J. van Stam, E. Moons, E. Cirillo, Quantitative analysis of phase formation and growth in ternary mixtures upon evaporation of one component, Phys. Rev. E 106 (2022) 025306.
[4] R. Lyons, S. Muntean, E. Cirillo, A. Muntean, A continuum model for morphology formation from interacting ternary mixtures: Simulation study of the formation and growth of patterns, Physica D 453 (2023) 133832.
[5] N. Khatamov, Holliday junctions in the Blume–Capel model of DNA, Theoret. Math. Phys. 206 (2021) 383–390.
[6] F. Graner, J. Glazier, Simulation of biological cell sorting using a two-dimensional extended potts model, Phys. Rev. Lett. 69 (1992) 2013–2016.
[7] A. Szabó, R. Merks, Cellular Potts modeling of tumor growth, tumor invasion, and tumor evolution, Front. Oncol. 3 (2013).
[8] E. Cirillo, E. Olivieri, Metastability and nucleation for the Blume-Capel model. different mechanisms of transition, J. Stat. Phys. 83 (3–4) (1996) 473–554.
[9] E. Cirillo, F. Nardi, Relaxation height in energy landscapes: an application to multiple metastable states, J. Stat. Phys. 150 (6) (2013) 1080–1114.
[10] C. Landim, P. Lemire, Metastability of the two–dimensional Blume–Capel model with zero chemical potential and small magnetic field, J. Stat. Phys. 164 (2016) 346–376.
[11] E. Cirillo, F. Nardi, C. Spitoni, Sum of exit times in a series of two metastable states, Eur. Phys. J. Spec. Top. 226 (10) (2017) 2421–2438.
[12] G. Bet, A. Gallo, F. Nardi, Critical configurations and tube of typical trajectories for the Potts and Ising models with zero external field, J. Stat. Phys. 184 (2021) 30.
[13] F. Manzo, E. Olivieri, Dynamical Blume–Capel model: competing metastable states at infinite volume, J. Stat. Phys. 104 (5–6) (2001) 1029–1090.
[14] C. Landim, P. Lemire, M. Mourragui, Metastability of the two–dimensional Blume–Capel model with zero chemical potential and small magnetic field on a large torus, J. Stat. Phys. 175 (2019) 456–494.
[15] F.D. Hollander, F. Nardi, A. Troiani, Kawasaki dynamics with two types of particles: critical droplets, J. Stat. Phys. 149 (6) (2012) 1013–1057.
[16] T. Fiig, B. Gorman, P. Rikvold, M. Novotny, Numerical transfer-matrix study of a model with competing metastable states, Phys. Rev. E 50 (1994) 1930–1947.
[17] Y. Yamamoto, K. Park, Metastability for the Blume–Capel model with distribution of magnetic anisotropy using different dynamics, Phys. Rev. E 88 (2013) 012110.
[18] P. Rikvold, B. Gorman, Recent results on the decay of metastable phases, Ann. Rev. Comput. Phys. 1 (1995) 149–191.
[19] M. Cassandro, A. Galves, E. Olivieri, M. Vares, Metastable behavior of stochastic dynamics: a pathwise approach, J. Stat. Phys. 35 (5–6) (1984) 603–634.
[20] E. Olivieri, E. Scoppola, Markov chains with exponentially small transition probabilities: first exit problem from a general domain I. The reversible case, J. Stat. Phys. 79 (3–4) (1995) 613–647.
[21] F. Manzo, F. Nardi, E. Olivieri, E. Scoppola, On the essential features of metastability: tunnelling time and critical configurations, J. Stat. Phys. 115 (1–2) (2004) 591–642.
[22] E. Cirillo, F. Nardi, J. Sohier, Metastability for general dynamics with rare transitions: escape time and critical configurations, J. Stat. Phys. 161 (2) (2015) 365–403.
[23] E. Olivieri, M. Vares, Large Deviations and Metastability, vol. 100, Cambridge University Press, 2005.
[24] P. Mathieu, P. Picco, Metastability and convergence to equilibrium for the random field curie–weiss model, J. Stat. Phys. 91 (1998) 679–732.
[25] A. Bovier, M. Eckhoff, V. Gayrard, M. Klein, Metastability and low lying spectra in reversible Markov chains, Comm. Math. Phys. 228 (2) (2002) 219–255.
[26] A. Bovier, F.D. Hollander, Metastability: A Potential-Theoretic Approach, vol. 351, Springer, 2016.

[27] J. Beltran, C. Landim, Tunneling and metastability of continuous time markov chains, J. Stat. Phys. 140 (6) (2010) 1065–1114.
[28] B. Cantor, Heterogeneous nucleation and adsorption, Trans. R. Soc. A 61 (2003) 409–417.
[29] J. Perepezko, W. Tong, Nucleation-catalysis-kinetics analysis under dynamic conditions, JSTOR 361 (2003) 447–461.
[30] V. Smorodin, P. Hopke, Relationship of heterogeneous nucleation and condensational growth on aerosol nanoparticles, Atmos. Res. 82 (3) (2006) 591–604.
[31] K. Binder, P. Virnau, Overview: Understanding nucleation phenomena from simulations of lattice gas models, J. Chem. Phys. 145 (21) (2016) 211701.
[32] A. Page, R. Sear, Heterogeneous nucleation in and out of pores, Phys. Rev. Lett. 97 (6) (2006) 065701.
[33] F. Restagno, L. Bocquet, T. Biben, Metastability and nucleation in capillary condensation, Phys. Rev. Lett. 84 (2000) 2433–2436.
[34] R. Sear, Metastability and nucleation in capillary condensation, J. Phys. Chem. B 110 (2006) 4985–4989.
[35] R. Sear, Formation of a metastable phase due to the presence of impurities, J. Phys.: Condens. Matter 17 (2005) 3997.
[36] E. Saridakis, N. Chayen, Towards a universal nucleant for protein crystallization, Trends Biotechnol. 27 (2009) 99–106.
[37] E. Curcio, V. Curcio, G.D. Profio, E. Fontananova, E. Drioli, Energetics of protein nucleation on rough polymeric surfaces, J. Phys. Chem. B 114 (43) (2010) 13650–13655.
[38] E. Cirillo, J. Lebowitz, Metastability in the two-dimensional Ising model with free boundary conditions, J. Stat. Phys. 90 (1–2) (1998) 211–226.
[39] G.B. Arous, R. Cerf, Metastability of the three dimensional Ising model on a torus at very low temperatures, Electron. J. Probab. 1 (1996).
[40] A. Bovier, F. Manzo, Metastability in Glauber dynamics in the low-temperature limit: beyond exponential asymptotics, J. Stat. Phys. 107 (3–4) (2002) 757–779.
[41] E. Cirillo, F. Nardi, C. Spitoni, Metastability for reversible Probabilistic Cellular Automata with self-interaction, J. Stat. Phys. 132 (3) (2008) 431–471.
[42] L. Alonso, R. Cerf, The three dimensional polyominoes of minimal area, Electron. J. Combin. 3 (1) (1996) R27.